

INVESTIGATION OF THE INJECTABILITY, CYTOTOXICITY, THERMAL
RESPONSE, AND DRUG RELEASE CAPABILITY OF DYNAMIC
POLY (ETHYLENE GLYCOL) HYDROGELS

by

Mackenzie Otakpor

HONORS CAPSTONE

Submitted to Texas State University
in partial fulfillment
of the requirements for
graduation in the Honors College
December 2023

Supervisor:

Tania Betancourt

Second Reader:

Adrienne Rosales

ABSTRACT

Hydrogels are versatile biomaterials composed of hydrophilic polymers that are cross-linked to form a network. Hydrogels are often used to mimic the extracellular matrix (ECM), which contains macromolecules that aid in the physical and chemical support of cells. In addition, they can be utilized as drug delivery systems, wound healing dressings, and materials for cell growth. In all these applications, the properties of the hydrogels must be tailored to match the distinct characteristics of various tissues in the body and to provide the function needed. For this reason, the hydrogel's stiffness, stress-relaxation properties, ability to present and release growth factors and therapeutic agents, cell encapsulation capabilities, and cytocompatibility must be optimized. Our collaborative group previously reported the development of dynamic poly (ethylene glycol) (PEG) hydrogels crosslinked via reversible thiol-Michael covalent bonds. The equilibrium nature of these bonds permits modulation of the properties of the hydrogels in response to changes in pH, temperature, and photothermal stimuli. Our laboratory is specifically interested in photothermal modulation of the hydrogels through the laser activation of entrapped poly(3,4-ethylenedioxythiophene) (PEDOT) nanoparticles since this provides the means to tailor the hydrogel's properties externally with spatiotemporal control and opens the doors to applications in on-demand drug delivery. The work herein described focuses on studying the factors that affect the hydrogel's injectability, cytocompatibility, stability, thermal response, and drug release capabilities. This thesis is broken up into two parts. One part focuses on the injectability, rheology, and cytocompatibility of dynamic hydrogels prepared with 4-arm PEG macromers with benzalcyanoacetamide end groups (PEG-RBCA) and 4-arm PEG macromers with thiol end groups (PEG-SH). The second part focuses on the thermal behavior,

stability, drug release, and cytocompatibility of more stable hydrogels including dynamic PEG-RBCA/PEG-SH crosslinks and nondynamic PEG-SH/PEG-Maleimide crosslinks.

ACKNOWLEDGEMENTS

I have many people to thank who have supported and guided me throughout my three years of research at Texas State University. I would like to first start off by thanking Dr. Jennifer Irvin who allowed me to join her lab during my sophomore year when I did not have very much research experience. I am grateful to Dr. Irvin for her patience, and encouragement, and for believing in my capabilities as a researcher. Additionally, I would like to extend my deepest gratitude to my research advisor, Dr. Tania Betancourt, for her amazing research guidance, insightful feedback, and continuous encouragement throughout my research endeavor. Working in her lab has provided me with invaluable connections between my academic coursework, research, and my future aspirations to become a doctor. I would also like to thank my second reader, Dr. Adrienne Rosales. I had the amazing opportunity to work in Dr. Rosales's lab during a summer REU with Andi Crowell, who was an excellent mentor. This opportunity broadened my exposure to a different research area, further enhancing my academic journey. Before attending Texas State University, research was not on my radar, and I had little knowledge about it. However, upon joining the PREM program under the guidance of Dr. Irvin and Dr. Betancourt, I was able to enter the research world. I've gained an array of insights and participated in several research conferences, experiences that pushed me beyond my comfort zone and broadened my horizons significantly. I would also like to thank the NSF Partnership for Research and Education in Materials (PREM) program (DMR-2122041) and the NSF Center for Dynamics and Control of Materials: an NSF MRSEC (DMR-1720595) for funding my research.

TABLE OF CONTENTS

	Page
ABSTRACT.....	2
ACKNOWLEDGMENTS	4
LIST OF FIGURES	7
CHAPTER	
1. INTRODUCTION	8
1.1. PEG-RBCA Project Overview	8
1.2. PEG-MAL Project Overview	9
1.3. Hydrogels in Biomedicine.....	9
1.4. Thermally and Photothermally Responsive Hydrogels.....	11
1.5. Hydrogel Injectability and Rheometry	13
2. RHEOMETRY, INJECTABILITY, AND CYTOCOMPATIBILITY OF PEG-RBCA/PEG-SH HYDROGELS	14
2.1. Materials.....	14
2.2. Preparation and Characterization of PEDOT NPs.....	15
2.3. PEG-RBCA Synthesis.....	16
2.4. PEG-RBCA Hydrogel Preparation.....	18
2.5. PEG-RBCA Hydrogel Rheometry	19
2.6. PEG-RBCA Hydrogel Injectability.....	20
2.7. <i>In Vitro</i> Model of Cytocompatibility.....	21
2.7.1. Cell Subculture Process for Studies	22
2.7.2. PEG-BCA MTS Assay (Cytocompatibility)	22
2.7.3. PEG-BCA Live/Dead Assay (Cytocompatibility).....	24
3. PEG-RBCA/SH RESULTS AND DISCUSSION	25
3.1. PEG-BCA Hydrogel Rheometry and Injectability	25
3.2. PEG-CBCA Hydrogel Rheometry and Injectability	26
3.3. PEG-BCA vs. PEG-CBCA.....	28
3.4. Cytocompatibility of PEG-BCA Hydrogels.....	39
4. CHARACTERIZATION AND CYTOCOMPATIBILITY OF PEG-MAL/BCA/SH HYDROGELS	32
4.1. Materials.....	32
4.2. Preparation and Characterization of PEDOT NPs.....	33
4.3. PEG-MAL Hydrogel Preparation.....	34
4.4. PEG-MAL Gel-to-Sol Temperature Study.....	37
4.5. PEG-MAL Drug Release Study	37
4.6. <i>In Vitro</i> Model of Cytocompatibility.....	38

4.6.1. Cell Subculture Process for Studies	39
4.6.2. PEG-MAL MTS Assay (Cytocompatibility).....	39
4.6.3. PEG-MAL Live/Dead Assay (Cytocompatibility).....	41
5. PEG-MAL/BCA/SH RESULTS AND DISCUSSION	43
5.1. PEG-MAL Gel-to-Sol Temperature Study.....	43
5.2. PEG-MAL Drug Release Study	45
5.3. Cytocompatibility of PEG-MAL Hydrogels	46
6. CONCLUSIONS AND FUTURE WORK	49
7. REFERENCES	51

LIST OF FIGURES

Figure	Page
1. Schematic of PEG-CA and PEG-RBCA Synthesis.....	17
2. Schematic of PEG-RBCA Hydrogel Formation	18
3. Rheometry Schematic	20
4. Syringe Pump Visual.....	21
5. PEG-BCA Rheometry and Injectability Data	26
6. PEG-CBCA Rheometry and Injectability Data.....	27
7. PEG-BCA vs. PEG-CBCA Comparison.....	28
8. PEG-BCA Cytocompatibility Data.....	30
9. Schematic of PEG-MAL Hydrogel Formation.....	34
10. Table of PEG-MAL Hydrogel Contents	35
11. Table of Amounts of PEG-MAL and Water for Stock Solutions.....	36
12. Table of PEG-MAL/SH/BCA Solution Prep for Hydrogel Assembly.....	36
13. Table of plate organization for MTS assay	40
14. PEG-MAL Gel-to-Sol Temperature Study Visuals.....	44
15. PEG-MAL Drug Release Data.....	46
16. PEG-MAL Cytocompatibility Data	47

1. INTRODUCTION

1.1 PEG-RBCA Project Overview

Hydrogels have found applications in biomedicine as tissue engineering scaffolds, wound healing materials, and drug delivery devices.¹ Dynamic hydrogels, specifically, contain crosslinks that can be modulated by a range of internal and external stimuli, making them uniquely suitable to changing tissue microenvironments or to the need for on-demand drug release. Specifically, dynamic hydrogels utilize crosslinks that are reversible in nature. In our collaborative work with the laboratory of Dr. Adrienne Rosales from The University of Texas at Austin, we have developed poly(ethylene glycol) (PEG) hydrogels that are crosslinked via dynamic covalent bonds that form through the thia-Michael addition reaction between 4-arm PEG macromers with benzalcyanoacetamide end groups (PEG-RBCA) and 4-arm PEG macromers with thiol end groups (PEG-SH).² PEG is a synthetic, biocompatible polymer that is highly customizable. The most recent work investigates the use of these hydrogels as drug delivery systems that can be activated, by virtue of their dynamic bonds, to release their cargo upon exposure to increased temperature.³ A drug delivery system that can be externally activated through photothermal modulation was developed by the incorporation of poly(3,4-ethylenedioxythiophene) (PEDOT) nanoparticles within these hydrogels. PEDOT nanoparticles absorb near-infrared light that can penetrate more deeply into tissues and convert it into heat within the hydrogels, thereby enabling on-demand activation. The first part of this thesis specifically focuses on how different PEG macromer molecular weights (10,000 and 20,000 g/mol) and conjugate acceptor (RBCA) identities affect the dynamic hydrogels' stiffness and injectability. It also examines the cytocompatibility of PEDOT nanoparticles, free PEG-RBCA

hydrogels, and PEDOT-loaded PEG-RBCA hydrogels in human breast cancer MDA-MB-231 cells and murine fibroblast 3T3 cells using the MTS cell viability and Live/Dead assays.

1.2 PEG-MAL Project Overview

Throughout the first set of studies of PEG-SH/PEG-RBCA hydrogels, it was noticed that, not surprisingly, the dynamic hydrogels show dissolution when exposed to excess fluids, leading to uncontrolled drug release. To address this issue while still trying to retain the dynamic nature of the hydrogels which enables on-demand alteration of the hydrogel's properties, a 4-arm-PEG-Maleimide (PEG-MAL) macromer was introduced as a secondary non-dynamic crosslink to restrain hydrogel dissolution and prevent unwanted drug release. This second section of the thesis specifically focuses on how PEG-MAL enhances the drug delivery aspects of the system as well as how it affects the cytocompatibility of the hydrogel.

1.3 Hydrogels in Biomedicine

Hydrogels, three-dimensional networks comprising crosslinked hydrophilic polymers derived from natural (collagen, hyaluronic acid, fibrinogen, chitosan) and synthetic (PEG, poly(methyl methacrylate), and poly(lactic-co-glycolic acid), poly(hydroxyethyl methacrylate)) materials, are highly attractive biomaterials in biomedicine.⁴ Their characteristics, including high water content, moderate mechanical properties, and tunable chemical and physical features, make them versatile for various applications. Hydrogels serve as biomimetic matrices for tissue regeneration and can encapsulate drugs, proteins, and cells. Depending on their composition, they can exhibit responsiveness to environmental triggers like water, pH, temperature, and ionic concentration, inducing changes in properties or disassembly. Common triggers, such as

hydrolysis, involve water molecules adding to the polymer backbone, causing the chain to break.⁴ Additionally, hydrogels can respond to stimuli like light or magnetic fields.⁴ In biomedicine, hydrogels can offer beneficial properties for applications in drug delivery, tissue engineering, regenerative medicine, and controlled release systems.

Hydrogels play a crucial role in biomedicine, particularly in drug delivery applications. These water-swollen networks, composed of hydrophilic polymers, find use in the controlled release of chemotherapeutic agents, peptides, and proteins.⁵ Hydrogels serve as bio-adhesive and mucoadhesive materials, adhering to mucosa or tissue for targeted drug delivery.⁵ In drug delivery, hydrogels, especially those containing polyethylene glycol (PEG), have been used to enhance the circulation half-life of drugs, reduce drug accumulation in clearance organs, and improve the biocompatibility of materials.⁶ Hydrogels have the capability of being able to noninvasively deliver proteins.⁷ Their glucose sensitivity can allow the hydrogel to respond to changes in glucose levels by releasing insulin.⁵ The development of hydrogels with specific properties, such as temperature or pH sensitivity, has expanded possibilities in drug delivery and tissue engineering. Hydrogels provide a versatile platform with unique properties for a range of biomedical applications.

For this thesis, PEG is used to formulate hydrogels. PEG is widely employed in the modification of peptides and proteins for various strategic reasons. One key benefit is the shielding of antigenic and immunogenic epitopes, effectively masking regions that might trigger an immune response.⁶ This not only reduces immunogenicity but also enhances the stability of peptides and proteins within the body. PEGylation, or the modification of proteins or biomaterials with PEG, serves to prevent the recognition and degradation of these biomolecules by proteolytic enzymes, thereby extending their half-life and overall therapeutic efficacy.⁶

Another advantageous aspect is the shielding of receptor-mediated uptake, preventing rapid clearance by the reticuloendothelial system (RES). This shielding effect contributes to prolonged circulation times, facilitating improved biodistribution.⁶ In essence, the incorporation of PEG enhances the pharmacokinetic properties of peptides and proteins, thereby augmenting their therapeutic potential.

1.4 Thermally and Photothermally Responsive Hydrogels

Thermally responsive hydrogels are materials with specific characteristics that make them especially useful in a variety of applications and are able to react to changes in temperature. These hydrogels can swell or contract in reaction to temperature changes, offering a dynamic and regulated response to the environment. Their ability to adjust the release rate of drugs or proteins based on temperature changes makes them helpful in applications like drug delivery, where they can be used to deliver precise and concentrated therapeutic effects. Temperature-responsive hydrogels exhibit distinct behaviors based on their response to temperature changes.⁸ One category comprises hydrogels demonstrating LCST (Lower Critical Solution Temperature) or UCST (Upper Critical Solution Temperature) behavior. For instance, polymers like poly(N-isopropyl acrylamide) (PNIPAAm) form hydrogels that are hydrophilic and swell below their LCST, around 32°C, but contract above this temperature due to increased hydrophobicity.⁸ In contrast, UCST hydrogel systems, involving hydrogen-bonded polymers like polyacrylamide and poly(acrylic acid), experience disrupted hydrogen bonds as the temperature rises, leading to hydrogel dissolution.⁸ Additionally, some hydrogels incorporate dynamic covalent bonds, where temperature modulates their equilibrium. With increasing temperature, the equilibrium of

exothermic reactions tends to shift towards the unbound state, while endothermic reactions shift towards increased bonding, affecting the overall behavior of the hydrogel system.⁸

External modulation of temperature-responsive hydrogels *in vivo* can be achieved through the use of photothermal stimuli. Photothermal agents capable of absorbing light and converting it into heat which are vital for photothermal therapy (PTT) often involve nanomaterials, specifically gold-based or silver-based nanostructures like nanoshells, nanorods, and nanoparticles.⁹ Poly(3,4-ethylenedioxythiophene) (PEDOT) nanoparticles are used in this thesis.^{10,11} Their effectiveness of photothermal agents lies in the strong absorption of light in the near-infrared (NIR) range and rapid energy conversion and dissipation.¹² In biomedical applications such as drug delivery, wound healing, and antitumor therapy, photothermal hydrogels encapsulate these agents into thermo-responsive matrices, offering advantages such as precise retention at desired sites, spatiotemporal control of cargo release, and prevention of nanoparticle aggregation.⁹

In the field of biomedicine, photothermally activated hydrogels have been used in a variety of ways, demonstrating their adaptability in solving numerous healthcare problems. These hydrogels have several notable applications, including on-demand medication delivery, where they work well as drug delivery systems. Drug release can be precisely timed and spatially induced by integrating photothermal agents into the hydrogel matrix, providing a controlled and targeted treatment strategy.⁹ Photothermal hydrogels have shown success in the treatment of infected wounds in the field of wound healing.⁹ The hydrogel's photothermal impact not only effectively kills bacteria but also speeds up the healing process.⁹ Additionally, photothermal hydrogels show potential in antitumor therapy in the field of cancer treatment.¹³ By minimizing harm to healthy tissues, the photothermal effect's localized hyperthermia enables the selective

killing of tumor cells.⁹ Photothermal hydrogels' accuracy, dynamic treatment capabilities, and ability to integrate many functional units, make them an interesting tool for different types of therapy in biomedicine.

1.5 Hydrogel Injectability and Rheometry

Tissues play a crucial role in providing the architectural framework for all tissues and organs in our bodies. Viscoelasticity, one of the mechanical characteristics of tissues, is crucial for understanding cellular mechanics and can be used to control cell behavior *in vitro*. A viscoelastic characteristic known as stress relaxation describes how a tissue's mechanical response changes over time as a result of deformation. There are so many different tissues in our body that each presents different stress relaxation properties. For instance, while heart valves have a slower relaxation rate and lower maximum stress relaxation, liver tissue can quickly relax a significant percentage of its stress.¹⁴ Understanding the ECM's mechanical characteristics, such as stiffness or elastic modulus, is essential for creating hydrogels that successfully interface with or resemble real tissues for biomedical use.

Hydrogels can be used as injectable materials for biomedical use because of the tunable properties that allow them to be formed and tailored to match whatever properties are needed for the intended tissue or application. To better understand the injectability and the mechanical compatibility of the hydrogels with the host tissue, we studied the rheological properties of the hydrogels and examined the injection force required for the administration of the hydrogels to make sure that it is clinically relevant.

2. RHEOMETRY, INJECTABILITY, AND CYTOCOMPATIBILITY OF PEG-RBCA/PEG-SH HYDROGELS

2.1. Materials

3,4-Ethylenedioxythiophene (EDOT) and chloroform were purchased from Alfa Aesar (Tewksbury, MA). Iron (III) chloride, anhydrous ethanol, poly(4-styrene sulfonic acid-co-maleic acid) sodium salt (PSS-co-MA), and dimethylformamide (DMF) were purchased from Sigma-Aldrich (St. Louis, MO). Methyl cyanoacetate and 4-dodecylbenzene sulfonic acid (DBSA) were purchased from TCI America (Portland, OR). Propargylamine, L-ascorbic acid sodium salt (or sodium ascorbate), and benzaldehyde were purchased from Beantown Chemical (Hudson, NH). Copper (II) sulfate and dimethyl sulfoxide-*d6* (DMSO-*d6*) were purchased from Acros Organics. 2kDa, 10kDa, and 100kDa dialysis bags were purchased from Spectrum Laboratories (Piscataway, NJ). 10X phosphate buffer saline (PBS) was purchased from KPL (Gaithersburg, MD). 4-arm-PEG_{10kDa}-azide, 4-arm-PEG_{20kDa}-azide, 4-arm-PEG_{10kDa}-thiol, and 4-arm-PEG_{20kDa}-thiol all were purchased from JenKem USA (Plano, TX). Bovine serum albumin (BSA) was purchased from Sigma-Aldrich (St. Louis, MO). Fluorescein isothiocyanate (FITC) was purchased from Thermo Fisher Scientific (Waltham, MA). BSA-FITC, a proteinic therapeutic mimic, was prepared by fluorescently labeling BSA with FITC by a student colleague with a previously reported protocol.¹⁵ Ultrapure water was obtained from a Millipore Direct-Q 3 system. MDA-MB-231 human breast cancer and 3T3 murine fibroblast cells were obtained from the American Type Culture Collection (ATCC) (Manassas, VA). 1x Dulbecco's phosphate-buffered saline (DPBS) and 100X penicillin-streptomycin solution were purchased from Corning (Manassas, VA). 1X Trypsin 0.25% solution and 1 M HEPES solution were purchased from Cytiva (Marlborough, MA). Fetal Bovine Serum (FBS) was purchased from RMBIO (Missoula,

MT). CellTiter 96[®] Aqueous One Solution Cell Proliferation (MTS) assay was purchased from Promega (Madison, WI). Live/Dead (Viability/Cytotoxicity) kit was purchased from Thermo Fisher Scientific (Waltham, MA). Methanol was purchased from VWR Chemicals (Radnor, PA).

2.2. Preparation and Characterization of PEDOT NPs

The poly(3,4-ethylenedioxythiophene) (PEDOT) nanoparticles (NPs) used in this thesis were prepared using an oxidative emulsion polymerization process and characterized using a Malvern Zetasizer and a Biotek Synergy spectrophotometer. For the preparation of the PEDOT NPs, the organic phase was made first by combining (0.09 g) 4-dodecylbenzene sulfonic acid (DBSA), (289.2 μ L) chloroform, and (10.8 μ L) 3,4-ethylenedioxythiophene (EDOT) in a microcentrifuge tube and vortexed/thermomixed at 2000 rpm at room temperature for 30 minutes (a color change from clear to dark red/black was observed). The aqueous phase was made next where (0.06 g) poly(4-styrene sulfonic acid-co-maleic acid) (PSS-co-MA) and (3 mL) ultrapure water were combined in a 20 mL glass vial with the addition of a small magnetic stir bar to help mix. Once the PSS-co-MA was mixed into the ultrapure water, the emulsion process began by adding the organic phase into the aqueous phase via a transfer pipette. This emulsion was left to mix for 5 minutes (a color change from black to green was observed). After 5 minutes, (6 mL) ultrapure water was then added to the vial to dilute the emulsion. The oxidant was made next by preparing a 100 mg/mL iron (III) chloride (FeCl₃) solution and combining (2.3-5 mg) FeCl₃ and (10 μ L for every mg of FeCl₃) ultrapure water together (a color change from black to orange occurred). The polymerization was then initiated by transferring 22.8 μ L of the FeCl₃ solution into the emulsion mixture and left to mix on the stir plate for 1 hour (leading to a color change from green to blue to black). The reaction was then transferred into a 100 kDA dialysis bag and

dialyzed against water for 14-17 hours. The dialyzed sample was then transferred into a glass vial for storage to conclude the preparation of the PEDOT NPs. After preparation, the NPs were then characterized with the Biotek Synergy spectrophotometer to identify the optical density in the visible/NIR and the peak absorption wavelength and then with a Malvern Zetasizer Nano ZS to analyze the size and the zeta potential of the NPs. The concentration and percent yield were also gathered after freeze-drying 2 mL of the NPs for two days with a Labconco FreeZone 4.5 lyophilizer.

2.3. PEG-RBCA Synthesis

To synthesize and purify the PEG-RBCA (Figure 1) polymer with molecular weights of 10,000 g/mol and 20,000 g/mol needed to be made first through copper-catalyzed click chemistry. PEG-CA was made by combining a (1 g) 4-arm-PEG_{10kDa}-azide or 4-arm-PEG_{20kDa}-azide and (58.6 mg) propargyl cyanoacetamide with a molar ratio of 4-arm-PEG-azide : propargyl cyanoacetamide of 1: 4.8 and then copper sulfate and sodium ascorbate with a molar ratio of PEG: (12.8 mg) copper sulfate: (31.7 mg) sodium ascorbate of 1:0.8:1.6. (8 mL) water and (8 mL) dimethylformamide (DMF) were also added and let react for 3 days. The mixture was then precipitated in (30 mL) ice-cold diethyl ether and centrifuged @12,000 rcf for 30mins @ 0°C so that the mixture separated into an aqueous layer and an organic layer. The organic layer was discarded, and the aqueous layer was put into a dialysis bag, dialyzed against water for 3 days, and then lyophilized for 3 days.

PEG-BCA was made by combining (272 mg) PEG-CA and (1110.2 µL) benzaldehyde with a molar ratio of PEG-CA: benzaldehyde of 1: 400 and (5 mL) anhydrous ethanol and letting react for 2 days. The mixture was then precipitated in diethyl ether (as described above) and then

placed in a vacuum oven overnight. The composition of the PEG-BCA polymer was confirmed by $^1\text{H-NMR}$.

PEG-CBCA was made by combining (272 mg) PEG-CA and (1426.7 mg) cyanobenzaldehyde with a molar ratio of PEG:CA: cyanobenzaldehyde of 1: 400 and (5 mL) anhydrous ethanol and letting react for 2 days. The mixture was then precipitated in diethyl ether and then placed in a vacuum oven overnight. The composition of the PEG-CBCA polymer was confirmed by $^1\text{H-NMR}$.

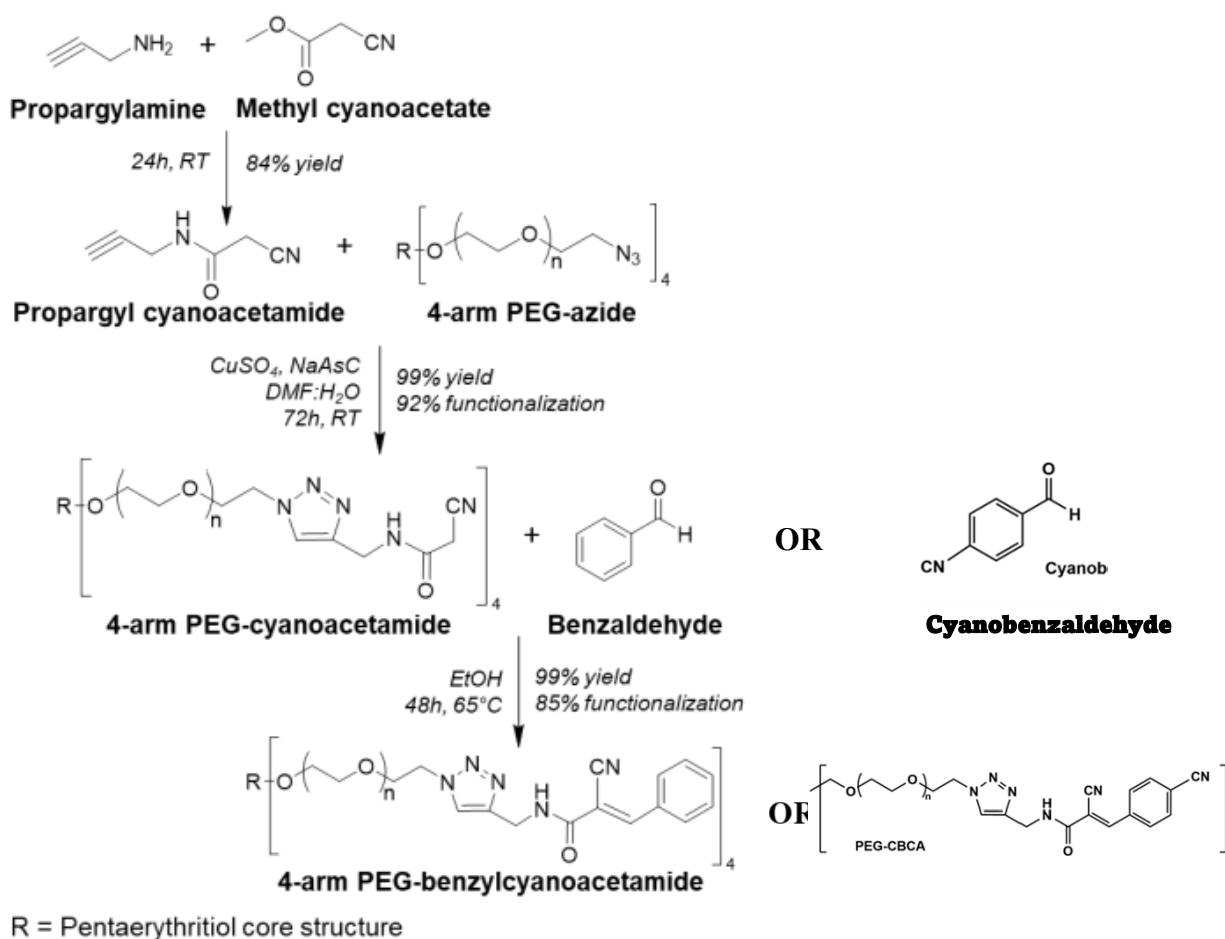


Figure 1. A schematic showing the synthesis of PEG-CA as well as PEG-RBCA. Two PEG macromers were functionalized with benzylcyanoacetamide acceptors. One contained the electron-withdrawing nitrile group in the para position of the aromatic (PEG-CBCA) and one without any aromatic substituents (PEG-BCA).

2.4. PEG-RBCA Hydrogel Preparation

The PEG-RBCA/SH hydrogels were prepared at room temperature through a thia-Michael addition reaction between 4-arm-PEG-RBCA and 4-arm-PEG-SH at a 1:1 molar ratio. PEG macromers (1.3 mg of PEG-RBCA and 1.2 mg of PEG-SH) of molecular weight 10,000 g/mol or 20,000 g/mol were mixed by hand in the presence of (5 μ L) phosphate-buffered saline (PBS) and (45 μ L) ultra-filtered water leading to gelation shortly after. For the preparation of photothermally activated hydrogels, 4-arm-PEG-RBCA and 4-arm-PEG-SH were mixed in the presence of PEDOT nanoparticles at a 1000 μ g/mL concentration (Figure 2). For the preparation of the hydrogels for drug delivery studies, 4-arm-PEG-RBCA and 4-arm-PEG-SH were mixed in the presence of PEDOT nanoparticles with a 1000 μ g/mL concentration and BSA-FITC with a 25 μ g/ μ L concentration.

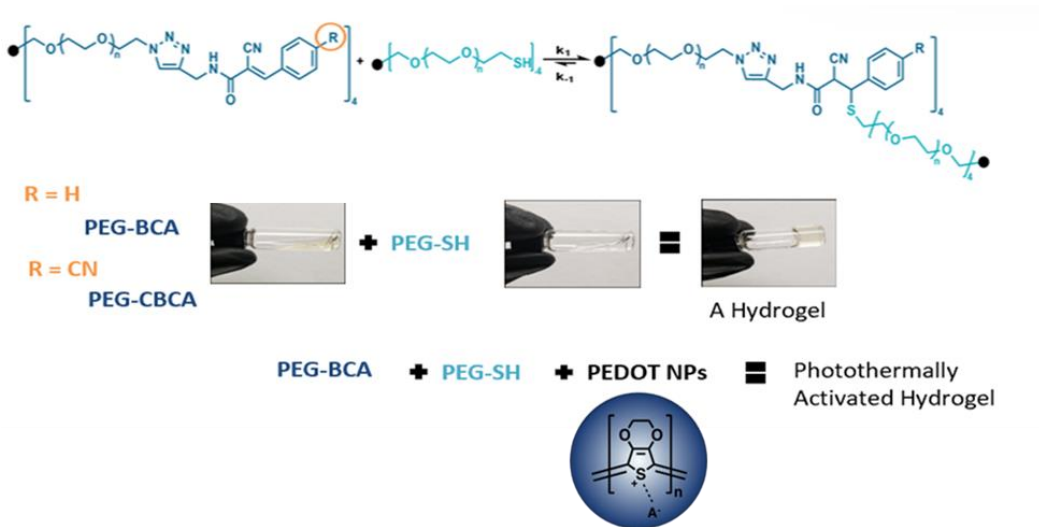


Figure 2. Hydrogel formation through the reaction between the conjugate acceptor-functionalized PEG shown in dark blue and a 4-arm PEG-thiol shown in light blue. Mixing the two precursor polymer solutions creates a dynamic hydrogel and the addition of PEDOT nanoparticles creates a photothermally activated hydrogel.

2.5. PEG-RBCA Hydrogel Rheometry

For this study, 2.75 wt%, 3.00 wt%, and 3.25 wt% concentrations of PEG-RBCA were utilized. When investigating the rheological properties of the PEG-RBCA/SH hydrogels, two methods were used. One method just required making the hydrogel on the rheometry plate while the other method required injecting the hydrogel directly onto the plate to investigate if the process of injecting the hydrogel would affect the hydrogel's properties. For the first method, 45 μL of each polymer solution (1.2 mg of PEG-RBCA and 1.1 mg of PEG-SH, 1:1 molar ratio) with molecular weights of 20,000 g/mol or 10,000 g/mol was pipetted onto the center of the Peltier plate of a TA Instruments Discovery HR2 rheometer with a 20 mm, 2° Cone without a Solvent Trap, and the polymer solutions were mixed together with a pipette tip until a gel formed. For the second method, 45 μL of each polymer solution (PEG-RBCA and PEG-SH) with molecular weights of 20,000 g/mol or 10,000 g/mol was pipetted onto a clean surface and mixed together with a pipette tip until a gel formed. The hydrogel was then transferred to a 0.5 mL insulin syringe with a 28 G needle to be injected onto the rheometry plate. For both methods, the rheometer geometry was then slowly lowered until the geometry made contact with the gel. Once the geometry made contact, it was then gradually lowered further to a gap height of 55 μm while the axial force was monitored (Figure 3). A pipette tip was then used to trim the edges of the gel to make the hydrogel diameter to be exactly the same as the geometry diameter and then the geometry was lowered to a gap height of 50 μm . Mineral oil was then added to the surroundings of the sample to prevent hydrogels from drying by losing water through the sides and then measurements began. The Peltier plate was set to 25 °C and the measurements that were focused on were a “Time Sweep” where a constant strain of 1% and constant frequency were applied, which made sure that the hydrogel properties were constant over the experimental time scale and

a “Frequency Sweep” where a constant strain of 1% was applied and the angular frequency was varied, which gave an insight into the plateau modulus and the stress-relaxation properties of the hydrogel.

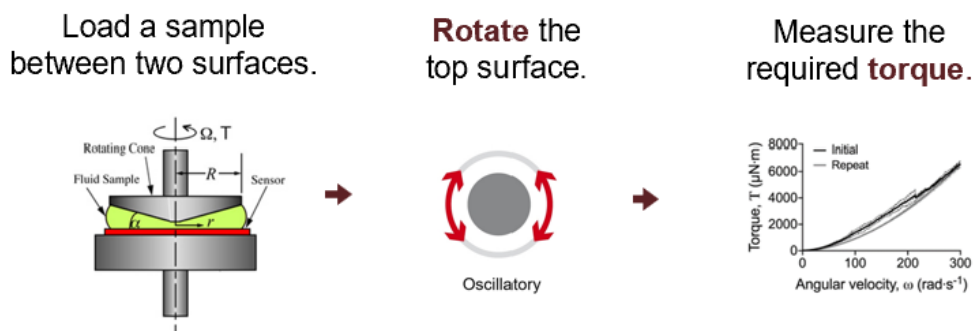


Figure 3. Visual representation of rheological experiments.^{16,17,18}

2.6. PEG-RBCA Hydrogel Injectability

The injectability of PEG-RBCA hydrogels was investigated to determine how much force is needed to extrude the hydrogels from a 28 G insulin syringe. PEG-RBCA with two different molecular weights (20,000 g/mol, 10,000 g/mol) was synthesized to figure out how the change in molecular weight affects the injectability of the hydrogel. For this study, load measurements were made in triplicates and a syringe pump (New Era Pump Systems model NE-300) with a load cell (FUTEK model LLB300) (Figure 4) was used along with the protocol described by Chen et al.¹⁹ PEG-RBCA and PEG-SH with molecular weights of either 20,000 g/mol or 10,000 were pipetted onto a clean surface and mixed together with a pipette tip until a gel formed. The gel that was made was then added to the cut end of a syringe and then centrifuged at 1000 rcf for 3 minutes to remove any bubbles that may have been present in the hydrogel. The gel was then transferred to a 0.5 mL insulin syringe with a 28 G needle and then the gel was pushed all the

way to the tip of the needle and then was left to rest in an upward position for 1 hour prior to being loaded onto the syringe pump. The syringe was then placed onto the syringe pump with the load cell placed behind the syringe plunger and the flow rate was set to 0.25 mL/min.

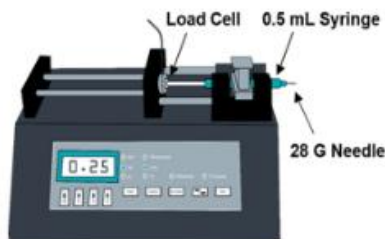


Figure 4. Visual representation of what the setup for collecting the injection force looked like.

2.7. *In Vitro* Model of Cytocompatibility

The cytocompatibility was measured through MTS viability and Live/Dead assays of cells exposed to hydrogel leachates. 5 wt% hydrogels were made by combining (1.2 mg) PEG-SH and (1.3 mg) PEG-BCA with a molecular weight of 10,000 g/mol in 1x PBS to make a 50 μ L gel. The gel was then incubated at 37°C for 24 hours in the presence of 1.3 mL of cell media. The media with hydrogel leachates was added to cells for 24 or 48 hours, as described below. The cell lines used were MDA-MB-231 cells which are an epithelial, human breast cancer cell line, and 3T3 cells which are a mouse embryonic fibroblast cell line. Cancer cells were used because of their ability to grow quickly, and they are easy to work with. Fibroblast cells were used because they are one of the most abundant types of cells found in humans and they make up a huge portion of the stromal tissue (connective tissue) in the human body which is important for wound healing. These cell lines were chosen with applications in cancer therapy, wound healing, and subcutaneous drug delivery in mind.

2.7.1. Cell Subculture Process for Studies

MDA-MB-231 cells were grown in media containing 88% Dulbecco's modified Eagle's medium (DMEM), 10% fetal bovine serum (FBS), 1% penicillin-streptomycin solution, 1% HEPES at 37 °C in a T-75 flask within a 5% CO₂ incubator. 3T3 cells were grown in media containing 89% (DMEM), 10% (FBS), and 1% HEPES at 37 °C in a T-75 flask. Cells were seeded when the T-75 flask reached 70-90% confluency. The cell media was removed from the T-75 flask, and the cells were rinsed with 2 mL of DPBS without Ca/Mg twice and then rinsed with 2 mL of Trypsin/EDTA. Next, the T-75 flask that contained the cells was placed in a 37 °C incubator with 5 mL of Trypsin/EDTA for 5 minutes to trypsinize. After 5 minutes, 5 mL of cell media was added to stop the trypsinization, and the cell suspension was put into a 15 mL tube and centrifuged at 125 rcf for 5 minutes. The cell media was removed without disturbing the cell pellet. The cell pellet was then resuspended in 5 mL of media for cell counting with a hemocytometer to figure out the correct dilutions for seeding cells into the 96-well plates for the studies. For both the MTS assay and the Live/Dead assay, the cells were seeded into a 96-well plate at 10,000 cells/well in 100 µL of media with 2 plates for the MTS assay (1 plate for the 24-hour study and 1 plate for the 48-hour study) and 2 plates for the Live/Dead assay (1 plate for the 24-hour study and 1 plate for the 48-hour study).

2.7.2. PEG-BCA MTS Assay (Cytocompatibility)

3-(4,5-dimethylthiazol-2-yl)-5-(3-carboxymethoxyphenyl)-2-(4-sulfophenyl)-2H-tetrazolium (MTS) assay is a colorimetric assay that is used to assess cell proliferation, cell viability, and cytotoxicity. The MTS assay is based on the reduction of the MTS tetrazolium reagent into a soluble formazan product by the action of dehydrogenase enzymes of

metabolically active cells. To perform the 24-hour and 48-hour MTS assays, two separate 96-well plates were prepared, one for the 24-hour study and one for the 48-hour study. On Day 1, the wells designated for cell seeding (5 by 5) were filled with 100 μ L of a solution mixture of a cell suspension mix (10,000 cells/well) and cell media, and the surrounding wells were filled with 100 μ L of DPBS and stored in a 37 $^{\circ}$ C incubator for 24 hours. Independent columns with five replicates each were specifically designated for different sample conditions. The preparation of the designated sample solutions begun on Day 1; these samples were stored for 24 hours in a 37 $^{\circ}$ C incubator. On day 2, after the cells were adhered to the bottom of the 96-well plate, the cell media was replaced with 100 μ L of the appropriate sample, as described next. On day 2, normal cell media was applied to column 1 and column 2. Column 1 was designated for the positive control (normal cell media) and column 2 was designated for the negative control (MeOH to induce cell death; MeOH was added on day 3 or 4). The other samples consisted of a 50 μ L hydrogel submerged in 1.3 mL of cell media to form the “Hydrogel” leachate (column 3), a sample with a 50 μ L hydrogel made with PEDOT NPs submerged in 1.3 mL of cell media to form “Hydrogel/PEDOT” leachate (column 4), and a sample with PEDOT NPs mixed with 1.3 mL of cell media (column 5, PEDOT sample). On Day 3 or 4 (after 24 or 48 hours of incubation with the treatment solutions), an MTS reagent solution consisting of 2500 μ L of DMEM and 500 μ L of MTS reagent was prepared. Negative control samples had their media removed and were exposed to MeOH for 30 min. The hydrogel leachates, or the media or MeOH for the controls, were replaced with 120 μ L of the MTS reagent, and the cells were stored in a 37 $^{\circ}$ C incubator for 2 hours. Subsequently, the absorbances of the samples were observed using the Biotek Synergy spectrophotometer at 490 nm. To calculate percent viability, the absorbance values were compared against the average of the positive control. The results were presented as the mean \pm

standard deviation among replicates. The statistical significance of the mean differences between the various sample tests and the positive control was determined using the student's t-test.

2.7.3. PEG-BCA Live/Dead Assay (Cytocompatibility)

The Live/Dead assay is a cell staining assay where live cells are stained with calcein and generate green fluorescence upon activation of calcein by enzymes in their cytoplasm and dead cells with compromised membranes are stained with the ethidium homodimer dye (EthD) which binds to their DNA and fluoresces red. To perform the 24-hour and 48-hour live-dead assays, two separate 96-well plates were prepared, one for the 24-hour study and one for the 48-hour study. The column and sample layout were the same as what was discussed for the MTS assay besides the fact that the Live/Dead assay only utilized two replicates while the MTS assay utilized 5 replicates. On Day 1, the wells designated for cell seeding (2 by 5) were filled with 100 μ L of a solution mixture of a cell suspension mix and cell media, and the surrounding wells were filled with DPBS and stored in a 37 $^{\circ}$ C incubator. On Day 2, the cells were adhered to the bottom of the 96-well plate, and the cell media was replaced with 100 μ L of its designated solution made on Day 1 and stored in a 37 $^{\circ}$ C incubator. On Day 3, a staining solution consisting of 1 μ L of calcein, 4 μ L of ethidium homodimer, and 2 mL of DPBS was prepared. The hydrogel leachates were then replaced with 100 μ L of the staining solution, and the cells were incubated at room temperature, covered with aluminum foil, for 30 minutes. After, the cells were observed using an EVOS FL fluorescence microscope, equipped with red fluorescent protein (λ EX 531/40 nm, λ EM 593/40 nm) and green fluorescent protein (λ EX 470/22 nm, λ EM 525/50 nm) filter cubes.

3. PEG-RBCA/SH RESULTS AND DISCUSSION

3.1. PEG-BCA Hydrogel Rheometry and Injectability

To evaluate the rheological properties of these hydrogels, time sweep, and frequency sweep measurements were conducted using a TA Instruments Discovery HR2 rheometer. The time sweep measurement was taken to make sure the gel properties are constant over the experimental time scale and the frequency sweep measurement was taken to give insight into the plateau modulus and the stress-relaxation of the gel. Rheometry results showed that as the molecular weight of the hydrogel precursors decreased (Figure 5A), the plateau modulus increased in gels having a total polymer concentration of 2.75, 3.00, and 3.23 wt%. The decreased macromer molecular weight results in a tighter network, resulting in a stiffer gel. In addition, the plateau modulus of the hydrogels generally decreased but stayed within range between the not injected and injected hydrogels (injected refers to the gel being pushed through a syringe onto the rheometry plate), supporting the reversibility of the gels as similar plateau moduli indicate that the injected hydrogels are able to self-heal into nearly equally crosslinked networks after injection. Finally, the PEG-BCA hydrogels showed an increase in injection force required as the molecular weight of the hydrogel precursors decreased (Figure 5B). This is again a result of the tighter network and increased crosslink density associated with the smaller molecular weight macromers.

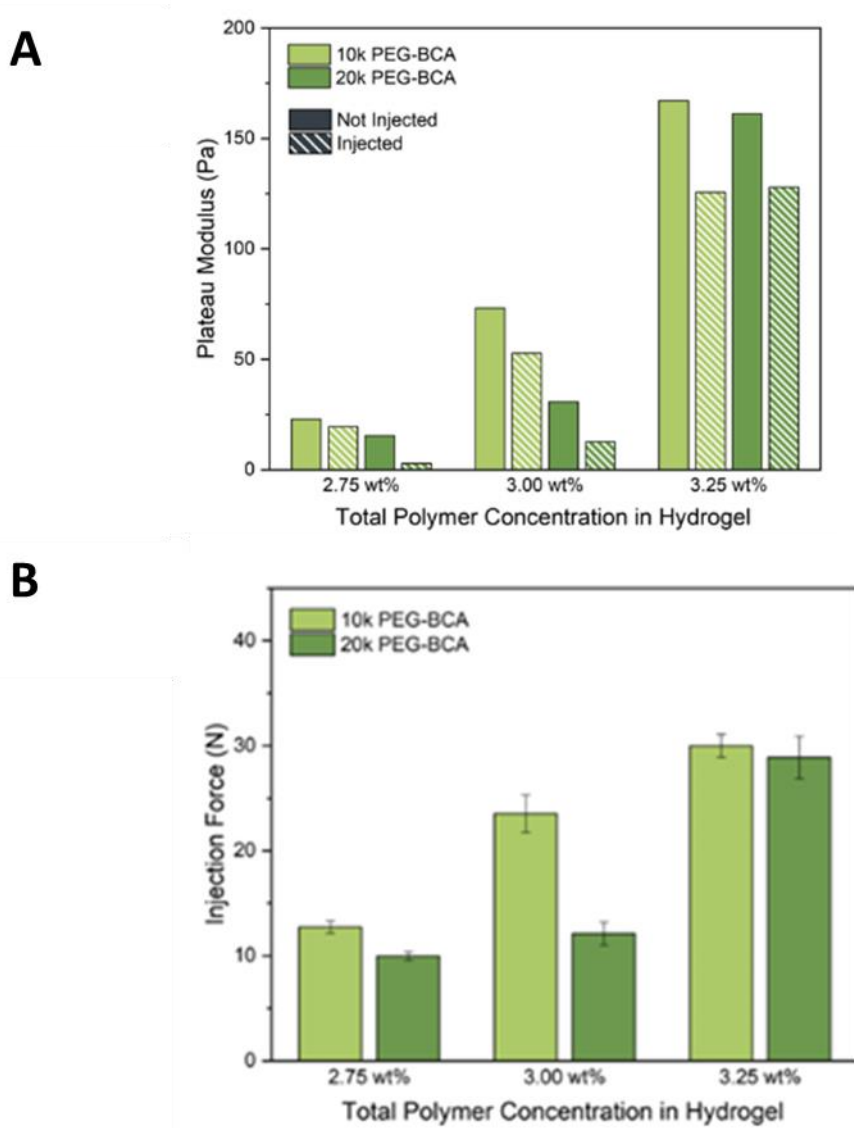


Figure 5. (A) Plateau modulus of PEG-BCA hydrogels obtained with a TA Instruments Discovery HR2 rheometer.

(B) Force required for injection of PEG-BCA hydrogels through a 28 G needle.

3.2. PEG-CBCA Hydrogel Rheometry and Injectability

As with PEG-BCA hydrogels, rheometry results showed that as the hydrogel precursors decreased in molecular weight, the plateau modulus increased in hydrogels with all polymer concentrations tested (Figure 6A). As mentioned above, the use of PEG macromers of smaller molecular weight results in a network with a higher crosslink density, resulting in a stiffer

material. In addition, the plateau modulus generally decreased but stayed within range between the not injected and injected hydrogels, again confirming the reversibility of the gels (injected refers to the gel being pushed through a syringe onto the rheometry plate). When evaluating the injectability properties, PEG-CBCA hydrogels showed an increase in injection force as the molecular weight of the PEG precursors decreased (Figure 6B).

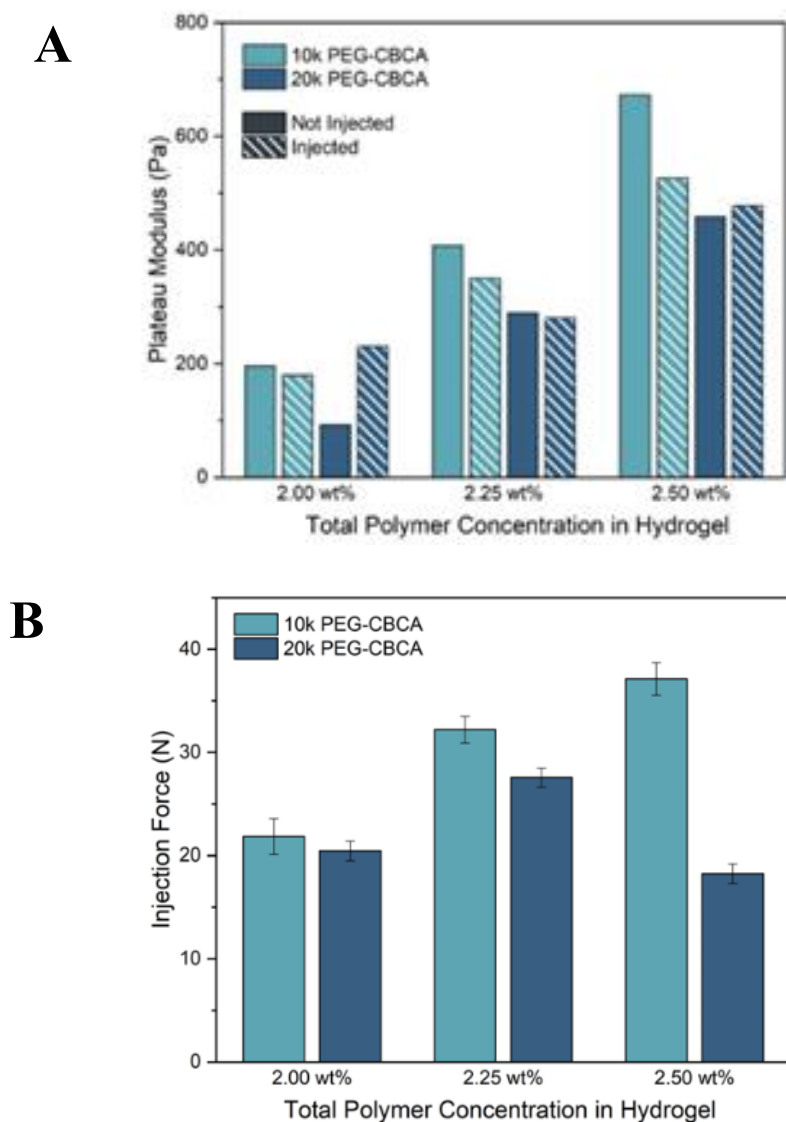


Figure 6. (A) Plateau modulus of PEG-CBCA hydrogels obtained with a TA Instruments Discovery HR2 rheometer. (B) Force required for injection of PEG-CBCA hydrogels through a 28 G needle.

3.3.PEG-BCA vs. PEG-CBCA

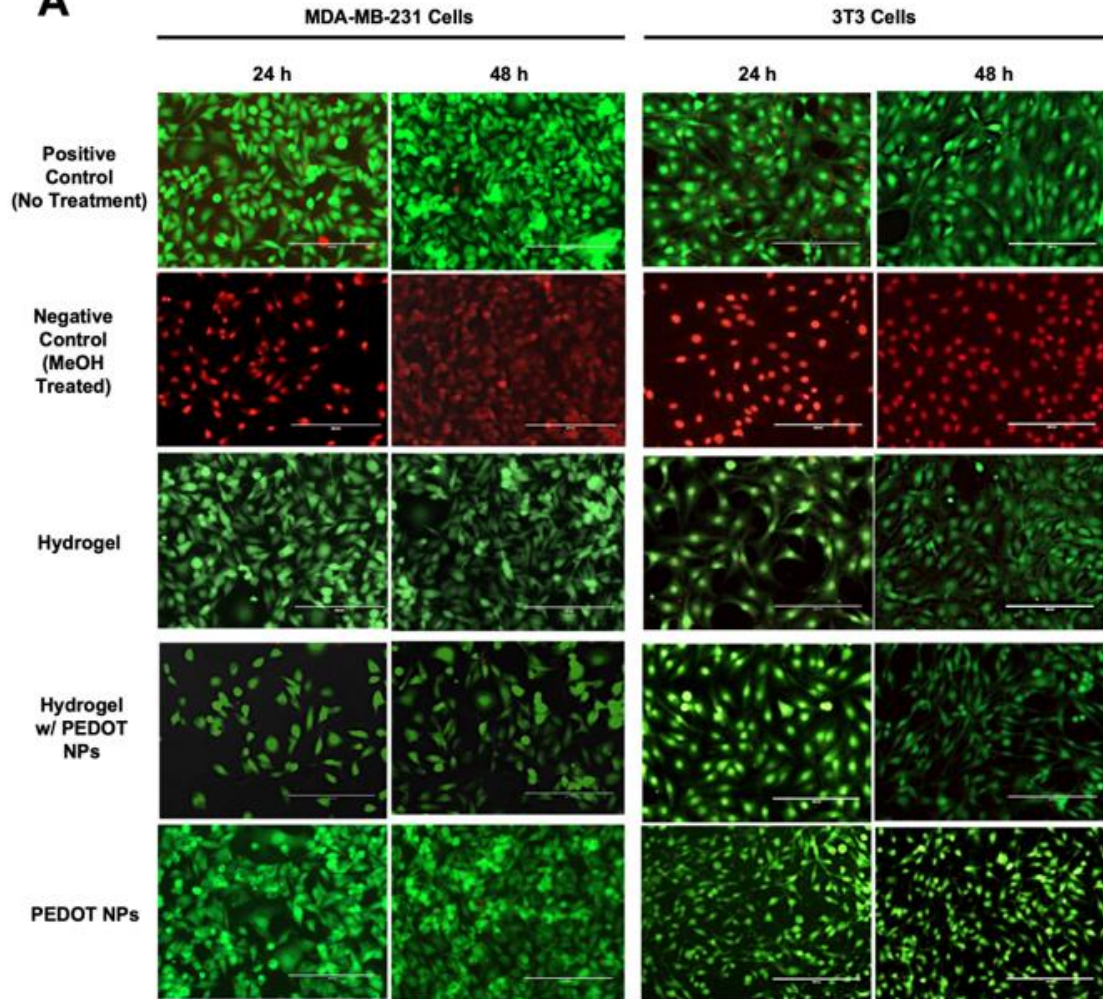
The distinctive properties of PEG-BCA and PEG-CBCA hydrogels, encompassing varying bond kinetics, gel stress-relaxation behaviors, and stiffness profiles, show their suitability for various applications. As shown in Figure 7 PEG-BCA hydrogels have slow bond kinetics and gel stress-relaxation properties as well as low stiffness (plateau moduli) (Figure 5A) while PEG-CBCA hydrogels have faster bond kinetics and gel stress-relaxation properties² as well as high stiffness (plateau moduli) (Figure 6A). While PEG-CBCA demonstrates faster reactivity compared to PEG-BCA, it remains relatively slow in relation to various other bond types, including hydrogen bonds, supramolecular bonds, and certain dynamic covalent bonds like boronic esters. The data shows the PEG-BCA hydrogel is more suitable for injection ability (Figure 5B) than the PEG-CBCA hydrogel (which requires a higher injection force) (Figure 6B) and that one can tune the injection force needed as well as stiffness by changing variables like the weight percentage and the molecular weight of the polymer. Furthermore, the data confirms the dynamic nature of these hydrogels, allowing their capability to self-heal into a cohesive structure post-injection. The data also opens the discussion for these hydrogel's capabilities for on-demand drug delivery, as the crosslinks display the capacity to self-repair after crosslink disruption, including after thermal disruption, holding substantial potential for therapeutic applications.

	PEG-BCA Hydrogel	PEG-CBCA Hydrogel
Bond Kinetics	SLOW	FAST
Stiffness (Plateau Modulus)	LOW	HIGH
Gel Stress-Relaxation	SLOW	FAST

Figure 7. The comparison of PEG-BCA and PEG-CBCA hydrogels in terms of bond kinetics, plateau modulus, and gel stress-relaxation.

3.4.Cytocompatibility of PEG-BCA Hydrogels

The Live/Dead and MTS assay studies allowed the cytocompatibility of the PEG-BCA hydrogels to be determined. In the Live/Dead assay it was expected that live cells would give off a green fluorescence upon the excitation of their cytoplasm if stained with calcein AM and dead cells would give off a red fluorescence from their nucleus if stained with ethidium homodimer dye (EthD) which binds to their DNA. Both the positive control (no treatment) and negative control (MeOH-killed) treatment samples gave us the results that were expected (Figure 8A) given that they were put in place to test the reliability of the experimental procedure. As shown in Figure 8A, there is no cell death from the samples that consisted of leachates from the hydrogel only, the hydrogel made with PEDOT NPs, and the PEDOT NPs only in both MDA-MB-231 and 3T3 cell lines. The MTS assay showed similar results from the Live/Dead assay where the data showed that the hydrogels do not decrease the viability of MDA-MB-231 breast cancer (Figure 8B) or 3T3 cells (Figure 8C). Both studies suggest that the PEG-BCA hydrogels have good potential as biomaterials for drug delivery applications.

A

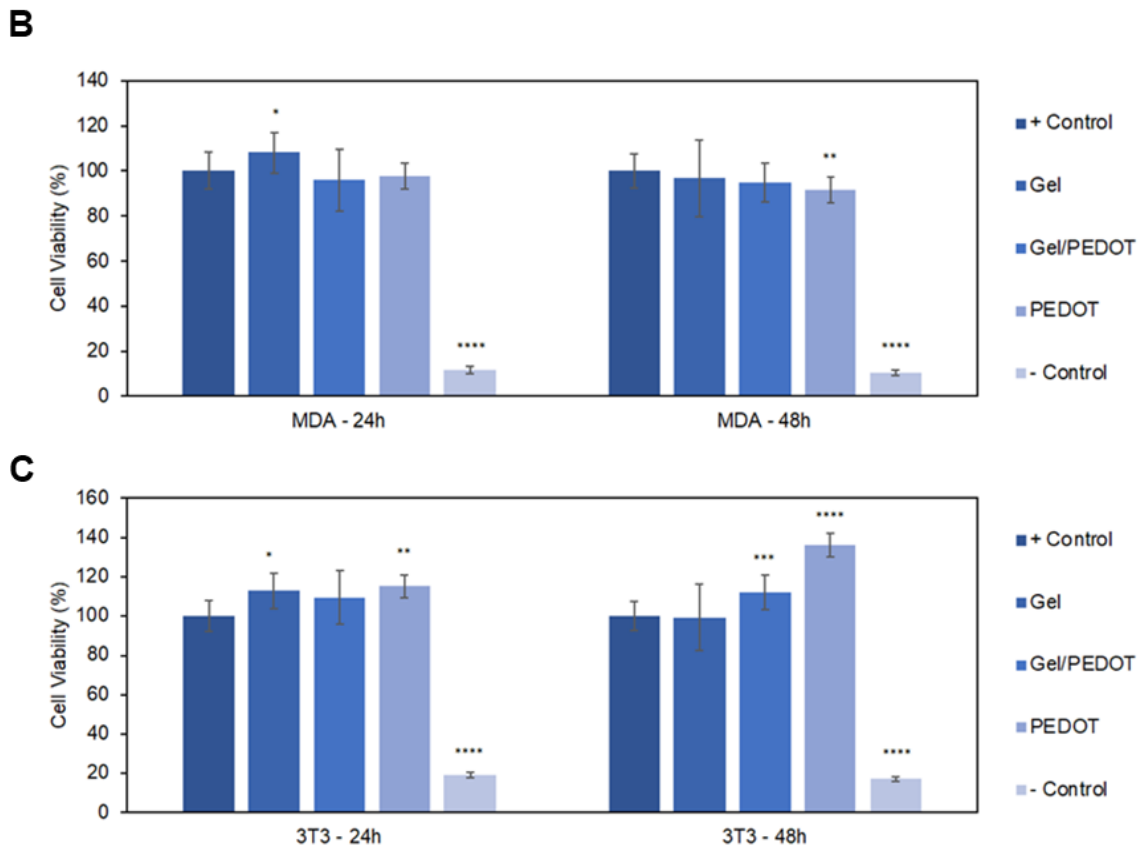


Figure 8. (A) Results of Live/Dead assay of MDA-MB-231 and 3T3 cell lines. Images are overlays of both green and red channels. Green fluorescence emits from metabolically active cells, while red fluorescence emits from dead cells that have a compromised cell membrane. Scale bar = 200 μ m. (B) Results of MTS assay of MDA-MB-231 cell line. (C) Results of MTS assay of 3T3 cell line. * p = 0.05, ** p = 0.01, *** p = 0.001, **** p = 0.0001.

4. CHARACTERIZATION AND CYTOCOMPATIBILITY OF PEG-MAL/PEG-BCA/PEG-SH HYDROGELS

4.1. Materials

3,4-Ethylenedioxythiophene (EDOT) and chloroform were purchased from Alfa Aesar (Tewksbury, MA). Iron(III) chloride, anhydrous ethanol, and dimethylformamide (DMF) were purchased from Sigma-Aldrich (St.Louis, MO). Methyl cyanoacetate and 4-dodecylbenzene sulfonic acid (DBSA) were purchased from TCI America (Portland, OR). Propargylamine, L-ascorbic acid sodium salt (or sodium ascorbate), and benzaldehyde were purchased from Beantown Chemical (Hudson, NH). Copper (II) sulfate and dimethyl sulfoxide-*d6* (DMSO-*d6*) were purchased from Acros Organics. 2kDa, 10kDa, and 100kDa dialysis bags were purchased from Spectrum Laboratories (Piscataway, NJ). 10X phosphate buffer solution (PBS) was purchased from KPL (Gaithersburg, MD). 4-arm-PEG_{10kDa}-azide, 4-arm-PEG_{10kDa}-thiol, and 4-arm-PEG_{10kDa}-MAL both were purchased from JenKem USA (Plano, TX). Bovine serum albumin (BSA) and poly(4-styrene sulfonic acid-co-maleic acid) sodium salt (PSS-co-MA) were purchased from Sigma-Aldrich (St.Louis, MO). Fluorescein isothiocyanate (FITC) was purchased from Thermo Fisher Scientific (Waltham, MA). BSA-FITC, a proteinic therapeutic mimic, was prepared by fluorescently labeling BSA with FITC by a student colleague with a previously reported protocol.¹⁵ Ultrapure water was obtained from a Millipore Direct-Q 3 system. Breast cancer and 3T3 cells were obtained from the American Type Culture Collection (ATCC) (Manassas, VA). 1x Dulbecco's phosphate-buffered saline (DPBS) and 100X penicillin-streptomycin solution were purchased from Corning (Manassas, VA). 1X trypsin 0.25% solution and 1 M HEPES solution were purchased from Cytiva (Marlborough, MA). Fetal Bovine Serum (FBS) was purchased from RMBIO (Missoula, MT). CellTiter 96® Aqueous One Solution Cell

Proliferation (MTS) assay was purchased from Promega (Madison, WI). Live/Dead (Viability/Cytotoxicity) kit was purchased from Thermo Fisher Scientific (Waltham, MA). Methanol was purchased from VWR Chemicals (Radnor, PA).

4.2. Preparation and Characterization of PEDOT NPs

The poly(3,4-ethylenedioxythiophene) (PEDOT) nanoparticles (NPs) used in this thesis were prepared using an oxidative emulsion polymerization process and characterized using a Malvern Zetasizer and a Biotek Synergy spectrophotometer. For the preparation of the PEDOT NPs, the organic phase was made first by combining (0.09 g) 4-dodecylbenzenesulfonic acid (DBSA), (289.2 μL) chloroform, and (10.8 μL) 3,4-ethylenedioxythiophene (EDOT) in a microcentrifuge tube. This mixture was vortexed/thermomixed at 2000 rpm at room temperature for 30 minutes (a color change from clear to dark red/black was visible). The aqueous phase was made next, where (0.06 g) poly(4-styrene sulfonic acid-co-maleic acid) (PSS-co-MA) and (3 mL) ultrapure water were combined in a 20 mL glass vial with the addition of a small magnetic stir bar to help mix. Once the PSS-co-MA was dissolved into the ultrapure water, the emulsion process began by adding the organic phase into the aqueous phase via a transfer pipette and was left to mix for 5 minutes (a color change from black to green was observed). After 5 minutes, (6 mL) ultrapure water was then added to the vial to dilute the emulsion. The oxidant was made next by preparing a 100 mg/mL iron (III) chloride (FeCl_3) solution and combining (2.3-5 mg) FeCl_3 and (10 μL for every mg of FeCl_3) ultrapure water together (a color change from black to orange occurred). The polymerization was then initiated by transferring 22.8 μL of the FeCl_3 solution into the emulsion mixture and left to mix on the stir plate for 1 hour (leading to a color change from green to blue to black). The reaction mixture was then transferred into a 100 kDA

dialysis bag and dialyzed against water for 14-17 hours, after which it was transferred into a glass vial for storage to conclude the preparation of the PEDOT NPs. After preparation, the NPs were then characterized with a Biotek Synergy spectrophotometer to identify the optical density and the peak absorption wavelength, and then a Malvern Zetasizer was used to get the size and the zeta potential of the NPs. The concentration and percent yield were also gathered after freeze drying 2 mL of the NPs for two days.

4.3. PEG-MAL Hydrogel Preparation

The macro polymers that are being used in this project are 4-arm poly(ethylene glycol) with benzylcyanoacetamide end groups (PEG-BCA), 4-arm poly(ethylene glycol) with maleimide end groups (PEG-MAL), and 4-arm poly(ethylene glycol) with thiol end groups (PEG-SH (thiol)) (Figure 9).

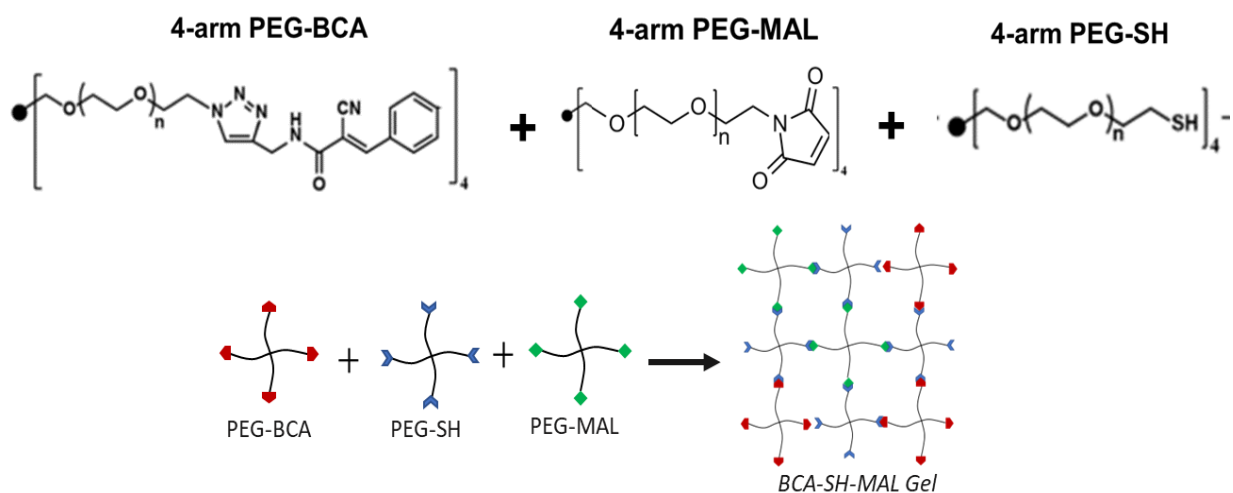


Figure 9. Hydrogel formation through the reaction between PEG-BCA/MAL/SH.

The PEG-MAL hydrogels were prepared at 5 wt% total polymer through a thia-Michael addition reaction in PBS with a molar ratio of 1:1 of PEG-BCA to the combination of PEG-SH/PEG-MAL and with the PEG-MAL representing 0, 1, 2.5, 5, 10, 100% (by moles) of the PEG-SH/PEG-MAL hydrogel system. For the preparation of photothermally activated hydrogels, PEG-BCA, PEG-MAL, and PEG-SH were mixed in the presence of PEDOT nanoparticles. Figure 10 presents the summary of ingredients used for the preparation of 50- μ L hydrogels of various PEG-MAL content (represented as % compared to mols of PEG-SH). The stock PEDOT and BSA-FITC concentrations used were 1.750 mg/mL and 225 mg/mL, respectively. The final concentration of these reagents in the hydrogel amounts to 1 mg/mL for PEDOT and 25 mg/mL for BSA-FITC.

PEG-MAL %	Dry Polymer (mg)			Solvent (μ L)			
	PEG-MAL	PEG-BCA	PEG-SH	PEDOT	BSA-FITC	10X PBS	Water
0	0	1.297	1.2	27.8	5.6	5	11.7
1	0.012	1.285	1.2	27.8	5.6	5	11.7
2.5	0.032	1.265	1.2	27.8	5.6	5	11.7
5	0.064	1.233	1.2	27.8	5.6	5	11.7
10	0.129	1.168	1.2	27.8	5.6	5	11.7
50	0.65	0.649	1.2	27.8	5.6	5	11.7
100	1.3	0	1.2	27.8	5.6	5	11.7

Figure 10. Final amounts of reactants used for the preparation of 50- μ L hydrogels with various PEG-MAL content. PEDOT refers to the PEDOT nanoparticle suspension stock of 1.75 mg/mL concentration. BSA-FITC refers to the 225 mg/mL stock solution of this fluorescently labeled protein.

Since the weight of PEG-MAL to be used in some of these formulations (specifically 1-50%) was very small, we made stock solutions of PEG-MAL (in water alone) for easier hydrogel assembly. Figure 11 shows the measurements used for these stock solutions.

% PEG-MAL	1	2.5	5	10	50	100
PEG-MAL (mg)	10	10	10	10	10	100
H ₂ O (μL)	3299.08	1319.63	659.82	329.91	65.982	329.91

Figure 11. Amounts of PEG-MAL and water used for preparation of PEG-MAL stock solutions for various formulations.

Then, just before hydrogel assembly, solutions of PEG-SH and PEG-BCA, as well as diluted solutions of PEG-MAL, were made, as shown in Figure 12, to make sure the polymers were thoroughly dissolved and homogeneously distributed in the final gel. Then, equal volumes of PEG-MAL, PEG-SH, and PEG-BCA were mixed (16.67μL each) to get a 50-μL hydrogel.

A

PEG-MAL %	PEG-MAL solution			
	PEG-MAL stock (μL)	PEDOT (μL)	BSA-FITC (μL)	10X PBS (μL)
0	0	0	0	0
1	3.9	9.25	1.85	1.65
2.5	3.9	9.25	1.85	1.65
5	3.9	9.25	1.85	1.65
10	3.9	9.25	1.85	1.65
50	3.9	9.25	1.85	1.65
100	5.85	13.90	2.80	2.50

B

PEG-MAL %	PEG-SH solution				
	PEG-SH (mg)	PEDOT (μL)	BSA-FITC (μL)	10X PBS (μL)	Water (μL)
0	1.2	13.9	2.8	2.5	5.85
1	1.2	9.25	1.85	1.65	3.9
2.5	1.2	9.25	1.85	1.65	3.9
5	1.2	9.25	1.85	1.65	3.9
10	1.2	9.25	1.85	1.65	3.9
50	1.2	9.25	1.85	1.65	3.9
100	1.2	13.9	2.8	2.5	5.85

C

PEG-MAL %	PEG-BCA solution				
	PEG-BCA (mg)	PEDOT (μL)	BSA-FITC (μL)	10X PBS (μL)	Water (μL)
0	1.297	13.9	2.8	2.5	5.85
1	1.285	9.25	1.85	1.65	3.9
2.5	1.265	9.25	1.85	1.65	3.9
5	1.233	9.25	1.85	1.65	3.9
10	1.168	9.25	1.85	1.65	3.9
50	0.649	9.25	1.85	1.65	3.9
100	0	0	0	0	0

Figure 12. (A) PEG-MAL, (B) PEG-SH, and (C) PEG-BCA solution preparations for hydrogel assembly.

4.4. PEG-MAL Gel-to-Sol Temperature Study

For this study, two 50- μL hydrogels containing BSA-FITC (for color) were made in glass vials for each sample type (0%, 1%, 2.5%, 5%, and 100% PEG-MAL), with one set of gels containing PEDOT NP and another other without PEDOT NP. The samples were examined at increasing temperatures (25, 40, 45, 50, 55, 60, and 65 $^{\circ}\text{C}$). For each temperature point, the vial was placed into a water bath for 5 min and then quickly taken out and placed upside down to see the effect the temperature had on the gel. A picture was taken immediately.

4.5. PEG-MAL Drug Release Study

For this week-long study, 5 replicates of 50- μL hydrogels containing BSA-FITC (the model drug) were made in microcentrifuge tubes for each sample type (0%, 1%, 2.5%, 5%, and 100% PEG-MAL). The hydrogels were then kept resting for 1 hour in a dark environment to reduce BSA-FITC photobleaching. After an hour, 1.3 mL of 1X PBS was added to the microcentrifuge tubes. Once about 1 minute had passed, 100 μL of the buffer solution was taken out from near the top of the tubes and was put in separate wells of a 96-well plate for

fluorescence reading. 100 μ L of the fresh buffer solution was then put back into the tubes and then the tubes were placed into a 37 °C water bath and the time was noted. The samples that were collected in the 96-well plate were run through fluorescence scanning at an excitation wavelength of 495 nm, emission wavelength of 525 nm, and a gain of 50, and the data was recorded. These same steps (drawing of 100 μ L of the buffer solution, replacement with fresh buffer, and reading of the fluorescence of the sample drawn) were followed every day for the rest of the week at the same time. A standard curve was used to determine the mass of BSA-FITC released at each time point.

4.6. *In Vitro* Model of Cytocompatibility

The cytocompatibility was measured through MTS and Live/Dead assays of cells exposed to hydrogel leachates. The hydrogels were made by combining both PEG-SH, PEG-MAL, and PEG-BCA to make a 50 μ L gel, as described above. The gel was then incubated at 37 °C for 24 hours in the presence of 1.3 mL of cell media. The media with hydrogel leachates was added to cells for 24 or 48 hours. The cell lines used were MDA-MB-231 cells which are an epithelial, human breast cancer cell line, and 3T3 cells which are a mouse embryonic fibroblast cell line. Cancer cells were used because of their ability to grow quickly, and they are easy to work with. Fibroblast cells were used because they are one of the most abundant types of cells found in humans and they make up a huge portion of the stromal tissue (connective tissue) in the human body which is important for wound healing. These cell lines were chosen with applications in cancer therapy, wound healing, and subcutaneous drug delivery in mind.

4.6.1. Cell Subculture Process for Studies

MDA-MB-231 cells were grown in media containing 88% Dulbecco's Modified Eagle's Medium (DMEM), 10% fetal bovine serum (FBS), 1% penicillin-streptomycin solution, 1% HEPES at 37 °C in a T-75 flask. 3T3 cells were grown in media containing 89% (DMEM), 10% (FBS), and 1% HEPES at 37 °C in a T-75 flask. Cells were subcultured and seeded for studies when the T-75 flask reached 70-90% confluency. The cell media was removed from the T-75 flask, and the cells were rinsed with 2 mL of DPBS without Ca/Mg twice and then rinsed with 2 mL of Trypsin/EDTA. Then, the T-75 flask that contained the cells was placed in a 37 °C incubator with 5 mL of Trypsin/EDTA for 5 minutes to trypsinize. After 5 minutes, 5 mL of cell media was added to stop the trypsinization, and the cell suspension was put into a 15-mL tube and centrifuged at 125 rcf for 5 minutes. The cell media was removed without disturbing the cell pellet and then the pellet was resuspended in 5 mL of media for cell counting with a hemocytometer to figure out the correct dilutions for seeding cells into the 96-well plates for the studies. For both the MTS assay and the Live/Dead assay, the cells were seeded into a 96-well plate at 10,000 cells/well in 100 μ L of media with 4 plates for the MTS assay (2 plates for the 24-hour study and 2 plates for the 48-hour study) and 2 plates for the Live/Dead assay (1 plate for the 24-hour study and 1 plate for the 48-hour study).

4.6.2. PEG-MAL MTS Assay (Cytocompatibility)

On Day 1, the wells designated for cell seeding (5 by 5) were filled with 100 μ L of a solution mixture of a cell suspension mix (10,000 cells/well) and cell media, and the surrounding wells were filled with 100 μ L of DPBS and stored in a 37 °C incubator for 24 hours. Independent columns with five replicates each were specifically designated for different sample conditions.

The preparation of the designated sample solutions began on Day 1; these samples were stored for 24 hours in a 37 °C incubator. On day 2, after the cells were adhered to the bottom of the 96-well plate, the cell media was replaced with 100 µL of the appropriate sample, as described next. On day 2, normal cell media was applied to column 1 and column 2. Column 1 was designated for the positive control (normal cell media) and column 2 was designated for the negative control (MeOH to induce cell death; MeOH was added on day 3 or 4). The other samples consisted of 50-µL hydrogels submerged in 1.3 mL of cell media to form the “Hydrogel” leachate samples, samples with 50-µL hydrogels made with PEDOT NPs submerged in 1.3 mL of cell media to form “Hydrogel/PEDOT” leachates, and a sample with PEDOT NPs mixed with 1.3 mL of cell media. Figure 13 summarizes the samples and their organization in the 96-well plates.

Plate A							
Column 1	Column 2	Column 3	Column 4	Column 5	Column 6	Column 7	Column 8
Positive Control	Negative Control	Leachate from 0% PEG-MAL Hydrogel	Leachate from 0% PEG-MAL Hydrogel with PEDOT NP	Leachate from 2.5% PEG-MAL Hydrogel	Leachate from 2.5% PEG-MAL Hydrogel with PEDOT NP	Leachate from 5% PEG-MAL Hydrogel	Leachate from 5% PEG-MAL Hydrogel with PEDOT NP

Plate B							
Column 1	Column 2	Column 3	Column 4	Column 5	Column 6	Column 7	Column 8
Positive Control	Negative Control	Leachate from 10% PEG-MAL Hydrogel	Leachate from 10% PEG-MAL Hydrogel with PEDOT NP	Leachate from 50% PEG-MAL Hydrogel	Leachate from 50% PEG-MAL Hydrogel with PEDOT NP	Leachate from 100% PEG-MAL Hydrogel	Leachate from 100% PEG-MAL Hydrogel with PEDOT NP

Figure 13. Plate organization for MTS assay.

On Day 3 or 4 (after 24 or 48 hours of incubation with the treatment solutions), an MTS reagent solution consisting of 2500 µL of DMEM and 500 µL of MTS reagent was prepared. Negative control samples had their media removed and were exposed to MeOH for 30 min. The hydrogel leachates, or the media or MeOH for the controls, were replaced with 120 µL of the

MTS reagent and the cells were stored in a 37 °C incubator for 2 hours. Subsequently, the absorbances of the samples were observed using the Biotek Synergy spectrophotometer at 490 nm. To calculate percent viability, the absorbance values were compared against the average of the positive control. The results were presented as the mean \pm standard deviation among replicates. The statistical significance of the mean differences between the various sample tests and the positive control were determined using the student's t-test.

4.6.3. PEG-MAL Live/Dead Assay (Cytocompatibility)

The Live/Dead assay is a cell staining assay where live cells are stained with calcein and generate green fluorescence upon activation of calcein by enzymes in their cytoplasm and dead cells with compromised membranes are stained with the ethidium homodimer dye (EthD) which binds to their DNA and fluoresces red. To perform the 24-hour and 48-hour live-dead assays, two separate 96-well plates were prepared, one for the 24-hour study and one for the 48-hour study. The column and sample layout were the same as what was discussed for the MTS assay besides the fact that the Live/Dead assay utilized no replicates while the MTS assay utilized 5 replicates. On Day 1, the wells designated for cell seeding (2 by 8) were filled with 100 μ L of a mixture of a cell suspension mix and cell media, and the surrounding wells were filled with DPBS and stored in a 37 °C incubator. On Day 2, the cells were adhered to the bottom of the 96-well plate, and the cell media was replaced with 100 μ L of its designated solution made on Day 1 and stored in a 37 °C incubator. On Day 3, a staining solution consisting of 5 μ L of calcein, 20 μ L of ethidium homodimer, and 10 mL of DPBS was prepared. The hydrogel leachates were then replaced with 100 μ L of the staining solution, and the cells were incubated at room temperature, covered with aluminum foil, for 30 minutes. After, the cells were observed using an EVOS FL fluorescence

microscope, equipped with a red fluorescent protein (λ_{EX} 531/40 nm, λ_{EM} 593/40 nm) and green fluorescent protein (λ_{EX} 470/22 nm, λ_{EM} 525/50 nm) filter cubes.

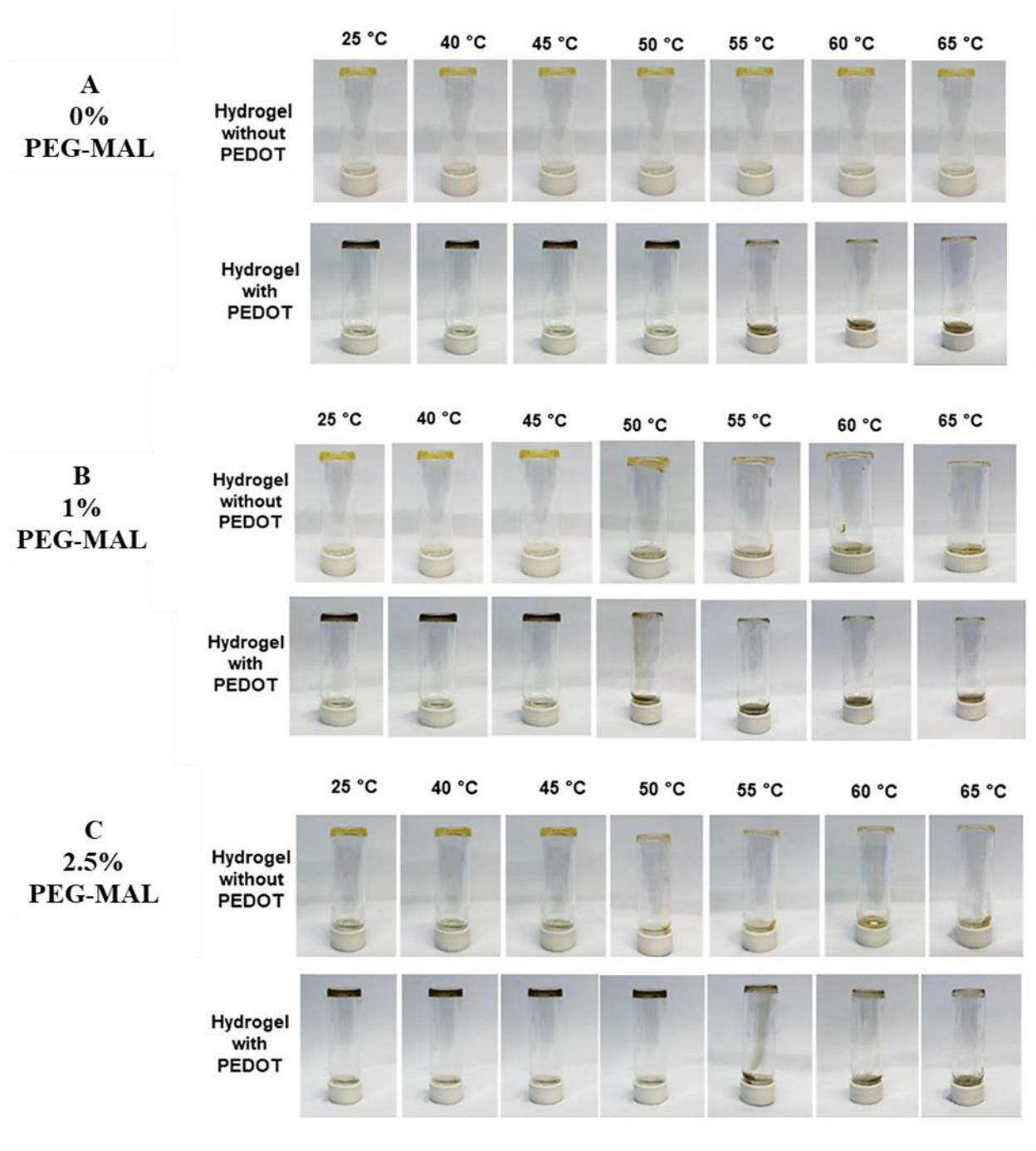
Further studies were carried out where cells were embedded within hydrogels and observed via confocal microscopy. To perform the Live/Dead assay with confocal microscopy, the hydrogel precursor solutions to make a 20- μ L 100% PEG-MAL hydrogel without PEDOT NPs were made and set aside. Then the cell pellet was made from cell subculture and was resuspended in 5 mL of cell media for cell counting with a hemocytometer to figure out the correct dilution to obtain 80,000 cells to encapsulate in the hydrogel. The correct cell dilution was then added into a 15 mL tube and 1 mL of cell media was added to the solution and then it was centrifuged at 125 rcf for 5 minutes. Once the cell pellet was formed the cell media was removed without disturbing the pellet and then the pellet was resuspended with one of the precursors. That cell pellet plus precursor mixture was added to an 8-well NuncTM Lab-TekTM II Chamber Slide System for confocal imaging. The other precursors were then added to the wells on top of the other precursor, gently pipetted to mix, and then stored in a 37 °C incubator until a gel formed. Once gelation took place, 300 μ L of media was added to the gel and placed into the incubator for 30 minutes. Next, a staining solution consisting of 1 μ L of calcein, 4 μ L of ethidium homodimer, and 2 mL of DPBS was prepared and then the cell media was replaced with the staining solution and was left to sit for 30 minutes. After the 30 minutes was over, the hydrogel was then ready to be imaged.

5. PEG-MAL/BCA/SH RESULTS AND DISCUSSION

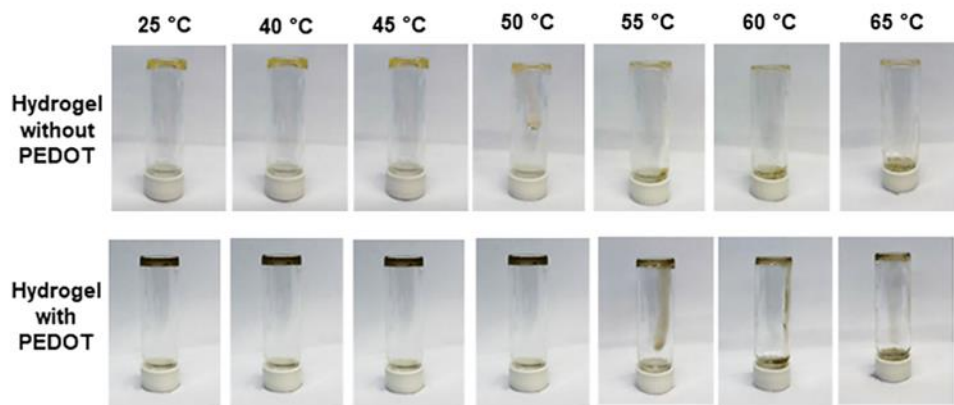
5.1. PEG-MAL Gel-to-Sol Temperature Study

Hydrogel gelation in the presence of PEG-MAL occurred similarly to that of the PEG-BCA/PEG-SH hydrogels described above. The inverted vial test was done to determine what temperature allowed the hydrogel to go from gel state to solution state (Figure 14). The 0% PEG-MAL hydrogels with and without PEDOT NPs did not display a transition when heated up to 65 °C for 5 minutes (Figure 14A). This result is unexpected and further replicates will be performed in the near future to ensure that the result is reproducible. The gel-to-sol transition temperature of the 1% PEG-MAL hydrogel without PEDOT NPs was between 45 °C and 50 °C while the gel-to-sol transition temperature of the 1% PEG-MAL hydrogel with PEDOT NPs was also between 45 °C and 50 °C (Figure 14B). The gel-to-sol transition temperature of the 2.5% PEG-MAL hydrogel without PEDOT NPs was between 45 °C and 50 °C while the gel-to-sol transition temperature of the 2.5% PEG-MAL hydrogel with PEDOT NPs was between 50 °C and 55 °C (Figure 14C). The gel-to-sol transition temperature of the 5% PEG-MAL hydrogel without PEDOT NPs was between 45 °C and 50 °C while the gel-to-sol transition temperature of the 5% PEG-MAL hydrogel with PEDOT NPs was between 50 °C and 55 °C (Figure 14D). The 100% PEG-MAL hydrogels with and without PEDOT NPs did not display a transition when heated up to 65 °C for 5 minutes (Figure 14E). This is due to the fact that PEG-MAL/SH bonds are thermally irreversible at physiologically relevant conditions. Given that this is a dynamic hydrogel, it is important to investigate the effects temperature has on the systems equilibrium. Because the PEG-BCA/PEG-SH reaction is exothermic, lower temperatures lead to an increased crosslinking, promoting a denser network structure, while higher temperatures lead to a reduction in crosslinking density. For medical applications, it is good to know if the hydrogel will work

well at body temperature or if it responds to things like fever or laser-targeted heating. Adjusting the hydrogel's properties to correlate with the results from the gel-to-sol temperature study will allow for a better and more efficient biomedical delivery system.



D
5%
PEG-MAL



(E)
100%
PEG-MAL

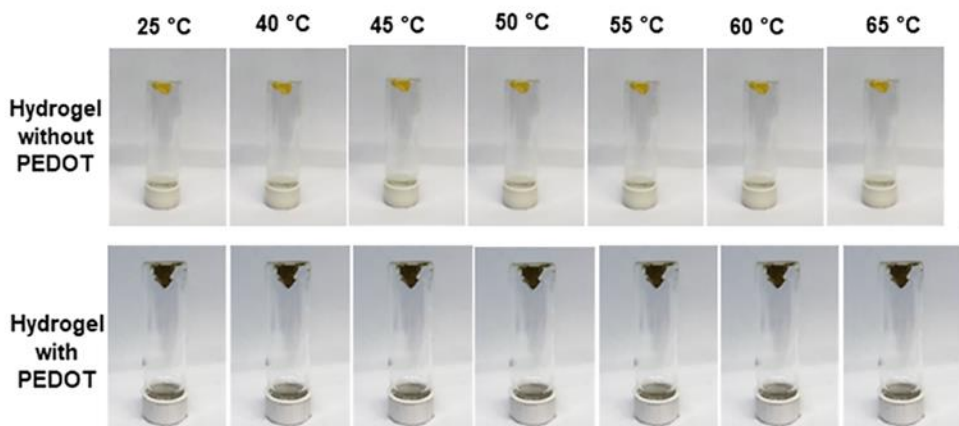


Figure 14. Inverted tube tests for (A) 0%, (B) 1%, (C) 2.5%, (D) 5%, and (E) 100% PEG-MAL with and without PEDOT NPs. Gel-to-sol transition is observed as the ability of the hydrogel components to flow down the tube when a high enough temperature is reached.

5.2. PEG-MAL Drug Release Study

Figure 15 shows the release of BSA-FITC from a 0% PEG-MAL hydrogel with PEDOT NPs and a 2.5% PEG-MAL hydrogel with PEDOT NPs while undergoing continuous thermal stimulation in a 37 °C water bath for a one-week time frame. One of the goals of adding PEG-MAL to the PEG-BCA/SH hydrogel system was to slow down the drug release over time. The results showed that PEG-MAL did show a decrease in drug release over time, but more studies need to be done to ensure the reproducibility of these data.

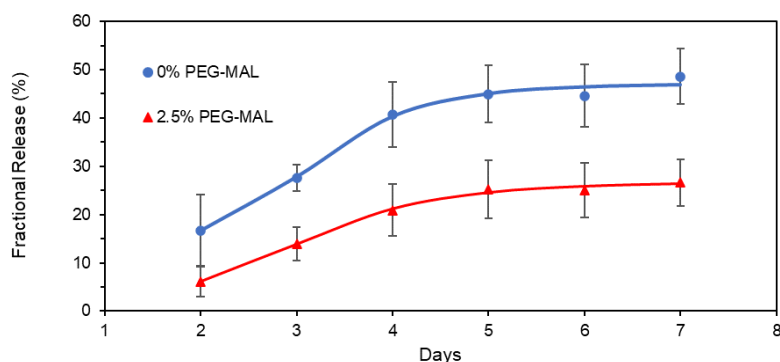


Figure 15. Drug release from a 0% and a 2.5% PEG-MAL hydrogel w/ PEDOT NPs under continuous thermal stimulation using a 37 °C water bath for a one-week time frame.

5.3. Cytocompatibility of PEG-MAL Hydrogels

As shown in Figure 16A, no cell death from the samples that consisted of leachates from hydrogels only is observed in the MDA-MB-231 cell line with the Live/Dead assay in 2-dimensional culture. The MTS assay (Figure 16B) showed similar results from the Live/Dead assay where the data suggest that the hydrogels do not decrease the viability of MDA-MB-231 breast cancer cells. As for the cell 3T3 cells we observed reduced viability (Figure 16B) with this cell line and one of the possibilities for this lower cell viability was the use of a different batch of PEDOT NPs.

Further studies were conducted by entrapping cells within hydrogels in situ. As shown in Figure 16 C and D, not only do cells exposed to leachates from the hydrogels fare well but also MDA-MB-231 cells entrapped within 100% PEG-MAL hydrogels also maintained viability. Specifically, cells were successfully entrapped within hydrogels by mixing them with the PEG-SH and PEG-MAL precursors and allowing the polymers to crosslink in the presence of the cells. Most cells showed green fluorescence, indicating good viability. The cells entrapped with the PEG hydrogel maintained a spherical cell morphology and this is because of their inability to

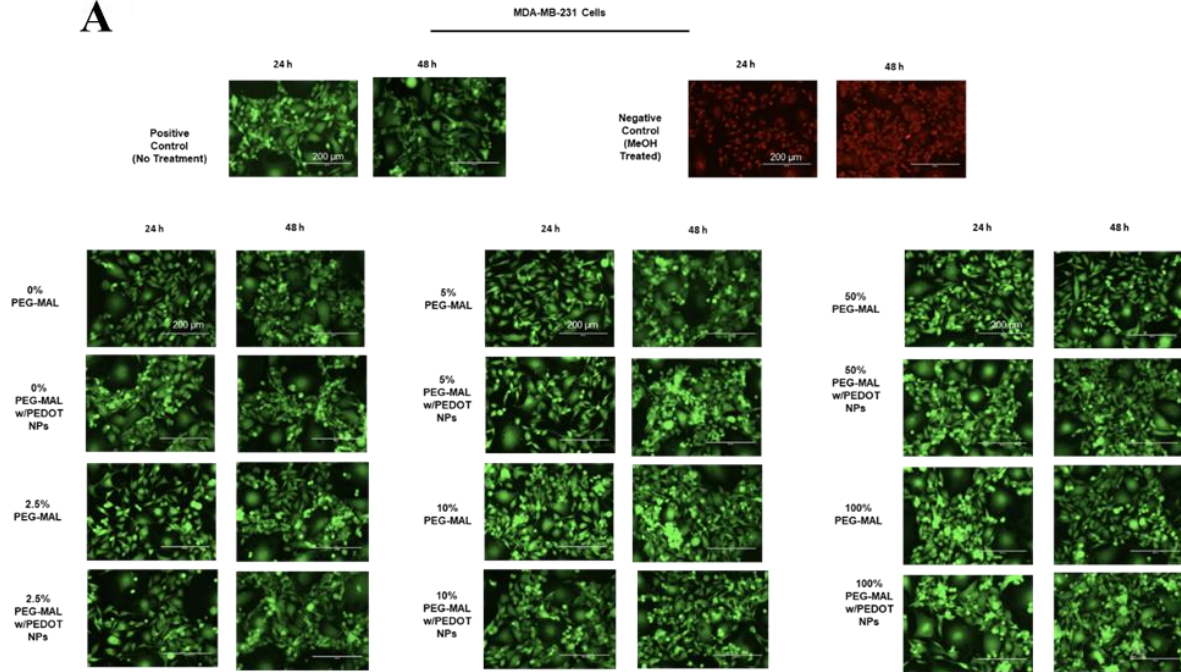
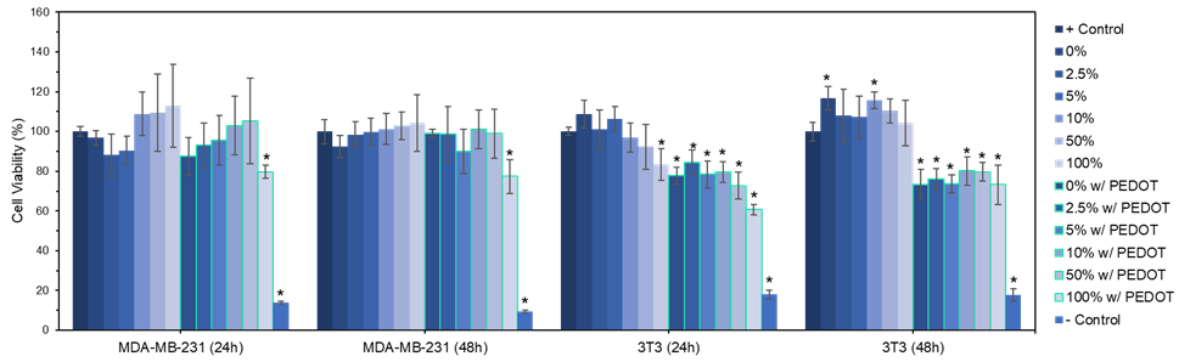
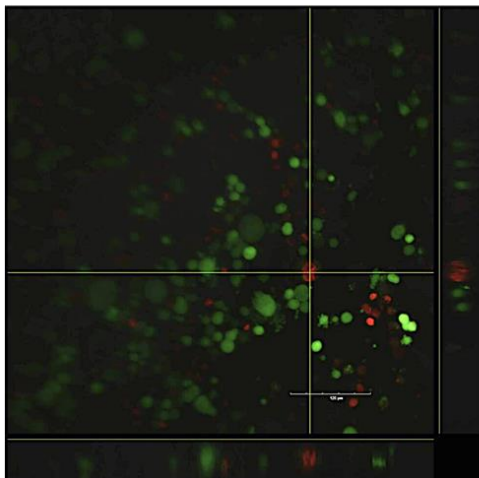
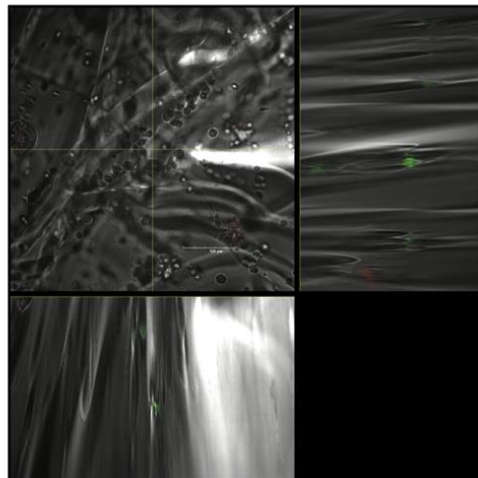
A**B****C****D**

Figure 16. (A) Results of Live/Dead assay of MDA-MB-231 cell line. Scale bar = 200 μm . (B) Results of 24-hr and 48-hr MTS assay of MDA-MB-231 cell line and 3T3 cell line. (C) Results of 48-hr MTS assay of MDA-MB-231 cell lines. (D) Confocal fluorescence (left) and differential interference contrast microscopy (DIC) (right) images of a 100% PEG-MAL hydrogel with MDA-MB-231 cells encapsulated within and stained with a Live/Dead assay reagent. Scale bar = 120 μm . Side and bottom panels on both left and right images represent the view along the depth of a three-dimensional hydrogel.

adhere to the hydrogel material that surrounds them. This lack of adhesion prevents the cells from spreading out as they would if they were in a T-75 flask or a 96-well plate, resulting in a consistent spherical morphology. As such, in general, all studies suggest that the PEG-MAL gels will not have any effect on cell viability without any other factors. Studies in 3T3 fibroblast cells for Live/Dead assay and with remaining PEG-MAL percentages will be conducted in the future.

6. CONCLUSIONS AND FUTURE WORK

In this thesis, the injectability, rheological properties, and cytocompatibility were investigated in PEG-RBCA/PEG-SH dynamic hydrogels, and the gel-to-sol transition temperatures, drug release profiles, and cytocompatibility were investigated in PEG-MAL/PEG-BCA/PEG-SH dynamic hydrogels. The results revealed that the molecular weight of the PEG-RBCA hydrogels influenced the mechanical properties of the hydrogels, with lower molecular weights leading to increased stiffness. The injectability of the hydrogels was affected by the molecular weight as well, with lower molecular weights requiring higher injection forces. Given that PEG-CBCA incorporates a nitrile a strong electron-withdrawing group while PEG-BCA incorporates a hydrogen, PEG-CBCA demonstrates a high plateau modulus and a higher injection force compared to PEG-BCA. The addition of PEG-MAL as a non-dynamic crosslinking agent improved the drug release aspect of the gel, allowing there to be a more controlled release of the drug, but more studies need to be carried out. However, in terms of the stability of the hydrogel, since the 0% PEG-MAL did not undergo gel-to-sol transition during the study for unknown reasons, the stability effect will need to be studied further.

Cytocompatibility studies using Live/Dead and MTS assays indicated that both PEG-RBCA/PEG-SH and PEG-MAL/PEG-BCA/PEG-SH hydrogels, with or without PEDOT nanoparticles, showed good biocompatibility with MDA-MB-231 breast cancer cells and 3T3 mouse fibroblast cells, although additional studies will need to be completed in 3T3 cells. The findings of this study contribute to the understanding of the factors influencing the performance of dynamic hydrogels in biomedical applications. The insights gained from this research can guide the further development and optimization of hydrogel-based drug delivery systems with

enhanced properties, providing a platform for future advancements in the field of biomaterials and biomedicine.

Future work on this project includes further exploring the effects of the addition of a 4-arm PEG-MAL on the hydrogel system as a whole. The next steps for this project would be to optimize the PEG-MAL ratio (1%, 2.5%, 10%, 50%, 100%) and, once that ratio has been determined, other studies will be done such as more drug release studies and biocompatibility studies, as well as investigation of the gelation kinetics, degradation behavior, mechanical attributes, self-healing capabilities, and injectability capabilities the PEG-MAL/BCA/SH hydrogel with and without PEDOT NP. These extensive analyses will offer a detailed understanding of how different concentrations of PEG-MAL affect the overall performance and properties of the hydrogel, guiding further refinements and applications of this biomaterial.

7. REFERENCES

1. Ho, T.-C.; Chang, C.-C.; Chan, H.-P.; Chung, T.-W.; Shu, C.-W.; Chuang, K.-P.; Duh, T.-H.; Yang, M.-H.; Tyan, Y.-C.. Hydrogels: Properties and Applications in Biomedicine. *Molecules* **2022**, 27 (9), 2902. <https://doi.org/10.3390/molecules27092902>.
2. Fitzsimons, T. M.; Anslyn, E. V.; Rosales, A. M. Effect of pH on the Properties of Hydrogels Cross-Linked via Dynamic Thia-Michael Addition Bonds. *ACS Polymers Au* **2022**, 2 (2), 129-136. DOI: 10.1021/acspolymersau.1c00049.
3. Kushal Thapa, Thomas M. FitzSimons, Mackenzie U. Otakpor, Mckenzie M. Siller, Anne D. Crowell, Joanna E. Zepeda, Edgar Torres, Lillian N. Roe, Jorge Arts, Adrienne M. Rosales, and Tania Betancourt *ACS Applied Materials & Interfaces* **2023** 15 (45), 52180-52196. DOI: 10.1021/acсами.3c11288
4. Deshayes, S., & Kasko, A. M. (2013). Polymeric biomaterials with engineered degradation. *Journal of Polymer Science Part A: Polymer Chemistry*, 51(17), 3531-3566. <https://doi.org/10.1002/pola.26765>
5. Langer, R., & Peppas, N. A. (2003). Advances in Biomaterials, Drug Delivery, and Bionanotechnology. *AIChE Journal*, 49(12), 2990–3006. <https://doi-org.libproxy.txstate.edu/10.1002/aic.690491202>
6. Fenton, O. S., Olafson, K. N., Pillai, P. S., Mitchell, M. J., & Langer, R. (2018). Advances in Biomaterials for Drug Delivery. *ADVANCED MATERIALS*, 30(29), 1705328. <https://doi-org.libproxy.txstate.edu/10.1002/adma.201705328>
7. Abune, L., & Wang, Y. (2021). Affinity Hydrogels for Protein Delivery. *Trends in pharmacological sciences*, 42(4), 300–312. <https://doi.org/10.1016/j.tips.2021.01.005>

8. Zeng, X., Liu, C., Fossat, M. J., Ren, P., Chilkoti, A., & Pappu, R. V. (2021). Design of intrinsically disordered proteins that undergo phase transitions with lower critical solution temperatures. *APL Materials*, 9(2), 1–13. <https://doi-org.libproxy.txstate.edu/10.1063/5.0037438>
9. Qian, Y., Lu, S., Meng, J., Chen, W., Li, J., Thermo-Responsive Hydrogels Coupled with Photothermal Agents for Biomedical Applications. *Macromol. Biosci.* 2023, 2300214. <https://doi-org.libproxy.txstate.edu/10.1002/mabi.202300214>
10. Huff, M. E.; Gökmen, F. Ö.; Barrera, J. S.; Lara, E. J.; Tunnell, J.; Irvin, J.; Betancourt, T. Induction of Immunogenic Cell Death in Breast Cancer by Conductive Polymer Nanoparticle-Mediated Photothermal Therapy. *ACS Applied Polymer Materials* **2020**, 2 (12), 5602-5620. DOI: 10.1021/acsapm.0c00938.
11. Cantu, T.; Walsh, K.; Pattani, V. P.; Moy, A.; Tunnell, J. W.; Irvin, J.; Betancourt, T.. Conductive Polymer-based Nanoparticles for Laser-mediated Photothermal Ablation of Cancer: Synthesis, Characterization, and in Vitro Evaluation. *International Journal of Nanomedicine* **2017**, Volume 12, 615–632. <https://doi.org/10.2147/ijn.s116583>.
12. Huang, X.; Jain, P. K.; El-Sayed, I. H.; El-Sayed, M. A.. Plasmonic Photothermal Therapy (PPTT) Using Gold Nanoparticles. *Lasers in Medical Science* **2008**, 23 (3), 217–228. <https://doi.org/10.1007/s10103-007-0470-x>.
13. Fu, Ji-Jun et al. “CuS Nanodot-Loaded Thermosensitive Hydrogel for Anticancer Photothermal Therapy.” *Molecular pharmaceuticals* vol. 15,10 (**2018**): 4621-4631. doi:10.1021/acs.molpharmaceut.8b00624

14. Tang, S., Richardson, B. M., & Anseth, K. S. (2021). Dynamic covalent hydrogels as biomaterials to mimic the viscoelasticity of soft tissues. *Progress in Materials Science*, 120, 100738. <https://doi.org/10.1016/j.pmatsci.2020.100738>
15. Roe, L. N. (2021). Functionalization of PEDOT nanoparticles for targeted delivery to cancer cells (Honors Thesis). Texas State University, San Marcos, Texas.
16. Kundu, P.; Kumar, V.; Scales, P. J.; Mishra, I. M.. Synergistic Influence of Ph and Temperature on Rheological Behavior of Adhesive Emulsions Stabilized with Micelle Dispersion of an Anionic Surfactant. *Journal of Surfactants and Detergents* **2019**, 22 (2), 301–313. <https://doi.org/10.1002/jsde.12220>.
17. Basics of rheology: Anton Paar Wiki. Anton Paar. (n.d.). <https://wiki.anton-paar.com/us-en/basics-of-rheology/>
18. Gloag, E. S.; Wozniak, D. J.; Wolf, K. L.; Masters, J. G.; Daep, C. A.; Stoodley, P.. Arginine Induced Streptococcus Gordonii Biofilm Detachment Using a Novel Rotating-disc Rheometry Method. *Frontiers in Cellular and Infection Microbiology* **2021**, 11. <https://doi.org/10.3389/fcimb.2021.784388>.
19. Chen, M. H.; Wang, L. L.; Chung, J. J.; Kim, Y.-H.; Atluri, P.; Burdick, J. A.. Methods to Assess Shear-thinning Hydrogels for Application as Injectable Biomaterials. *ACS Biomaterials Science & Engineering* **2017**, 3 (12), 3146–3160. <https://doi.org/10.1021/acsbomaterials.7b00734>.